universität wien

MASTER'S THESIS

Title of the Master's Thesis

„Mechanism of transcription cooperativity by signal transducers and activators of transcription and NFκB"

submitted by

Christophe Capelle

in partial fulfilment of the requirements for the degree of

Master of Science (MSc)

Vienna, 2016

degree programme code as it appears on the student record sheet:	A 066 830
degree programme as it appears on the student record sheet:	Masterstudium Molekulare Mikrobiologie, Mikrobielle Ökologie und Immunbiologie
Supervisor:	Univ.-Prof. Dr. Thomas Decker

universität wien

MASTERARBEIT

Titel der Masterarbeit

„Mechanism of transcription cooperativity by signal transducers and activators of transcription and NFκB“

verfasst von

Christophe Capelle

angestrebter akademischer Grad

Master of Science (MSc)

Wien, 2016

Studienkennzahl lt. Studienblatt:	A 066 830
Studienrichtung lt. Studienblatt:	Masterstudium Molekulare Mikrobiologie, Mikrobielle Ökologie und Immunbiologie
Betreut von:	Univ.-Prof. Dr. Thomas Decker

Acknowledgements

First of all I would like to thank my supervisor Prof. Thomas Decker for giving me the opportunity to work on this project. Also, thank you for all the science-related and -unrelated things that you have taught me during this time.

Many thanks go to my lab mates: Andrea, Roland, Duygu, Daniel, Sebastian, Felix and Fabian, who made it fun to come to work every day. I would especially like to thank Katrin for the excellent supervision and support during the thesis, but also for the many laughs that we shared. You all contributed to a great working atmosphere and made these times unforgettable.

I would also like to thank the Baccarini, Kovarik and Versteeg lab for always being kind and helpful.

Many thanks go to the Ogris Lab, for the patience and guidance during the generation and testing of the monoclonal antibody.

I particularly want to thank my friends and flatmates Rasha, Max and Xavier for the support and the memorable times that we shared during our studies.

A very special thanks goes to old friends that I know for the greater part of my life and to my new friends that I met during my studies in Innsbruck and Vienna, who helped to shape me into who I am today.

I also particularly want to thank my parents and sister for the everlasting support, advice and encouragement. I would not be where I am, without you showing me the right way.

Finally, a warm thanks to my grandparents for always being proud of me and despite the distance, always providing me with motivational chocolate during the exams.

Table of contents

Introduction

Innate Immunity

Upon invasion of host organisms by an infectious pathogenic agent, a plethora of complex interactions between the host immune system and the pathogen start to unfold. While the skin or mucosal epithelia act as the first line of defence, the innate immune system is initiated by the recognition of evolutionary conserved pathogen associated molecular patterns (PAMP) by host pattern recognition receptors (PRR) expressed on specialized cells of the innate immune system, such as dendritic cells, macrophages and neutrophils. This recognition triggers a variety of signaling cascades, which work together to fight the infection by inducing an inflammatory response mediated by cytokines and chemokines. However, this does not lead to an efficient clearance of the pathogen or a long-lasting immunity against this pathogen. Instead, phagocytic cells of the innate immune system, particularly dendritic cells (DCs) [2], present antigens to the cells of the adaptive immune system, thus initiating an effective adaptive immune response through the generation of pathogen-specific B- and T lymphocytes. These cells are necessary for the production of antigen-specific antibodies and the elimination of infected cells. Only a tight cooperation between the innate and adaptive immunity allows an effective clearance of the pathogen [1].

Pattern recognition

The detection of microbial patterns is mediated by pattern recognition receptors (PRR), expressed on the cell surface, within endosomes or the cytoplasm of innate immune cells. So far, several classes of PRR, such as Toll-like receptors (TLR), Nod-like receptors (NLR), RIG-I-like receptors (RLR) and cytosolic DNA sensors have been identified and characterized [3]. These receptors are able to sense different classes of molecules including carbohydrates, lipoproteins, glycolipids, proteins of the bacterial cell wall and nucleic acid structures originating from both extracellular and intracellular pathogens. This recognition is necessary to mount an appropriate immune response to a pathogen [3, 4].

Toll-like receptors (TLR)

TLRs have been widely studied and represent a major class of PRR, counting 10 members in humans and 13 in mice [4]. They are considered to be the primary sen-

sors of pathogens. TLRs are type I membrane glycoproteins and are composed of an extracellular LRR (leucine-rich repeat) domain, a transmembrane domain and a cytoplasmic TIR (Toll/IL-1 receptor) domain [5]. The LRR domain is involved in the recognition of different PAMPs, whereas the intracellular TIR domain mediates the initiation of downstream signaling by recruitment of TIR domain-containing adaptor proteins, such as MyD88 (myeloid differentiation primary response gene 88), TIRAP (TIR-containing adaptor protein), TRIF (TIR-containing adaptor-inducing IFN-β) and TRAM (TRIF-related adaptor molecule). Broadly, TLR signaling can be divided into MyD88-dependent and TRIF-dependent pathways. Depending on which adaptor proteins are recruited, pathways leading to the activation of the transcription factors NF-κB (nuclear factor κB), IRFs (IFN regulatory factors) and AP1 (activator protein 1) are initiated, culminating in the production of inflammatory cytokines and type I IFN [2, 3]. TLRs are expressed on the cell surface (TLR1, TLR2, TLR4, TLR5 and TLR6) as well as in the endosomes (TLR3, TLR7, TLR8 and TLR9) of a variety of different immune and non-immune cells, such as macrophages, dendritic cells, B-cells, natural killer (NK) cells, fibroblasts, epithelial cells and endothelial cells [2].

NOD-like receptors (NLR)

The NOD-like receptor (NLR) family, comprising 23 members in humans and 34 in mice, sense a wide range of ligands within the cytoplasm of cells, including PAMPs and danger-associated molecular patterns (DAMPs). Members of the NLR share structural and functional characteristics.

The C-terminal domain contains leucine rich repeats (LRR) and is important for the recognition of ligands. The N-terminal domain, involved in the recruitment of adaptor proteins required for downstream signaling, harbours different domains, such as the caspase recruitment domain (CARD), the Pyrin domain (PYD), the death effector domain (DED) or baculovirus inhibitor repeats (BIRs). The intermediate domain consists of nucleotide-binding and oligomerization (NACHT) domains [6].

The NLRs NOD1 and NOD2 recognize common components of bacterial cell walls, such as peptidoglycan, muramyl dipeptide (MDP) and dipeptide g-D-glutamyl-meso-diaminopimelic acid (iE-DAP) from various microbial pathogens such as *Listeria monocytogenes* [7]. Recognition by NLRs triggers the activation of NFκB and MAP kinases to induce the production of inflammatory cytokines. Other members of the

NLR family, such as NLRP1, NLRP3, IPAF and AIM2 are components of the inflammasome, thus involved in the activation of inflammatory caspases [8, 9].

Rig-I-like receptors (RLR)

The RIG-I-like receptors are members of the DExD/H RNA helicase family and function as cytosolic sensors for viral RNA [10]. To date, 3 members of the RLR have been identified: RIG-I (retinoic acid-inducible gene I), MDA5 (melanoma differentiation associated factor 5), and LGP2 (laboratory of genetics and physiology 2). All members of the RLR family share structural similarities. [10, 11] They display a common repressor domain (RD) at their C-terminus, which is involved in the regulation of RIG-I-dependent downstream signaling. Furthermore they harbour an intermediate ATP-dependent DExD/H-box RNA helicase domain, required for ligand binding. RIG-I and MDA5, but not LGP2 contain an N-terminal CARD domain, necessary for downstream signaling [11]. LGP2 is currently thought to function as a positive regulator for RIG-I and MDA5 [12], but was initially found to negatively regulate RIG-I and MDA5 [13].

RLR family members have been implicated in the recognition of several different families of RNA viruses [14]. However, RIG-I recognizes ssRNA with a 5' triphosphate or short dsRNA, whereas MDA5 only recognizes long dsRNA without any 5' phosphorylation [14]. Additionally, RIG-I has been shown to detect nucleic acids originating from bacteria, such as *Listeria monocytogenes* [15]. Viral RNA is recognized in the cytoplasm by RIG-I or MDA5, which leads to an ATP-dependent conformational change of the sensors [16], exposing the CARD domains to enable an interaction with CARD-containing adaptors, such as the mitochondrial activator of virus signaling (MAVS) [10]. MAVS is mainly located to the mitochondria, but also to peroxisomes and mitochondrial-associated endoplasmic reticulum (ER) membrane (MAM) [17]. Peroxisomal MAVS induces an early response through the induction of interferon-stimulated genes (ISGs) via IRF1, whereas mitochondrial MAVS induces a delayed response via IRF3 [18]. Upon activation, RIG-I and MDA5 associate with MAVS through their CARD domain, to further activate the Ser/Thr kinases TBK1 and IKKε. These are in turn responsible for the activation of IRF3, IRF7 and NFκB. Upon activation these transcription factors translocate to the nucleus to induce the transcription of proinflamatory genes, direct antiviral genes and interferons, which in turn induces the

transcription of interferon-stimulated genes (ISG) via the JAK/STAT signaling pathway.

Cytosolic DNA sensors

DNA was known to trigger innate immune responses long before its sensors were identified. TLR9, mainly expressed in plasmacytoid dendritic cells (pDC) and B cells, is known to recognize endosomal CpG DNA, produced by bacteria and viruses, which leads to the production of type I interferons [20, 21]. However, cells lacking TLR9 or a RLR are still able to induce the production of type I interferons [22]. This indicates the existence of alternative mechanisms for DNA sensing.

The first identified cytosolic DNA sensor, DNA-dependent activator of IFN-regulatory factors (DAI), binds cytosolic dsDNA and leads to the production of type I IFNs through IRF3 and TBK1 [23]. Not only the production of type I interferons, but also of the proinflamatory cytokines IL-1β and IL-18 was observed following dsDNA recognition. Absent in melanoma 2 (AIM2), a member of the hematopoietic interferon-inducible nuclear protein HIN-200 family, was identified as a cytosolic DNA sensor involved in the activation of the inflammasome through the interaction with ASC, leading to the cleavage of caspase-1 and secretion of IL-1β and IL-18 [24].

In 2008, Stimulator of Interferon Genes (STING), an ER-bound adaptor protein, was identified as critical for the production of type I interferons after exposure to DNA-based pathogens or a variety of DNA types [25, 26]. However, the mechanism how STING is activated by cytosolic DNA remained unclear until recently. STING was identified to directly associate with dsDNA and cyclic dinucleotides (CDN), a second messenger secreted by intracellular bacteria, such as *Listeria monocytogenes* [21]. Additionally, cyclic-GMP-AMP (cGAMP) synthase (cGAS), was identified as a DNA sensor that synthesises the cyclic dinucleotide cGAMP in a DNA-dependent manner, which then bind to and activate STING [27]. Upon activation, STING recruits TBK1 and IKK to phosphorylate IRF3 and IκBα, respectively. IRF3 dimers and NFκB are now able to translocate to the nucleus to induce the production of type I interferons and inflammatory cytokines [28].

In the past, several other DNA sensors inducing the production of type I interferons have been identified, including RNA polymerase III, LRRFIP1, DHX9, DHX36, IFI16

and DDX41 [29, 30].

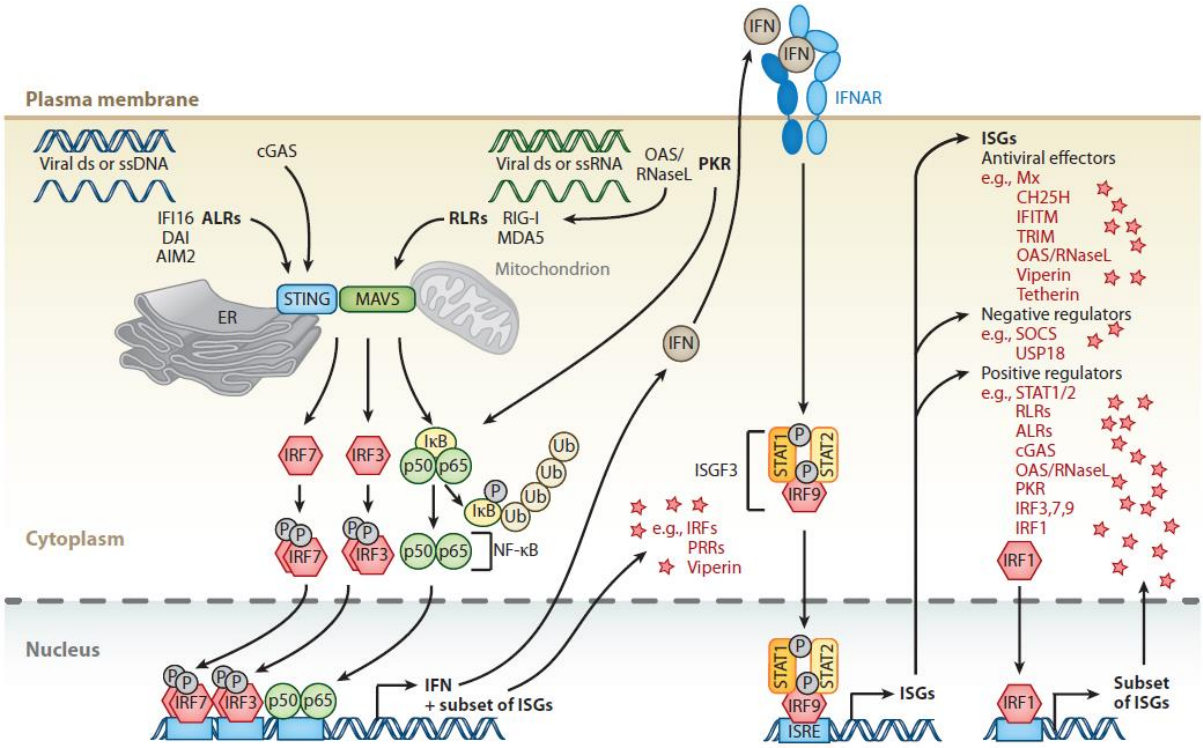

Figure 1: Cytosolic nucleic acid pattern recognition and activation of ISGs. Specialized PRRs recognize foreign DNA or RNA and transduce the signal to transcription factors through STING and MAVS, respectively. Activation of STING or MAVS leads to the phosphorylation-induced activation of transcription factors. Once active, they translocate to the nucleus where they bind to and activate specific promoters, triggering the expression and secretion of type I interferon (IFN-I). In turn, IFN-I bind to their receptor and induce the phosphorylation of STAT1 and STAT2 through JAKs and assembly of the ISGF3 complex, resulting in the expression of multiple interferon stimulated genes. [37]

Interferons in innate immunity

Interferons (IFNs) are a family of cytokines best known for inducing a cell-intrinsic antiviral state in infected and neighbouring cells [31]. However, they have numerous additional functions that regulate both innate and adaptive immunity. IFNs also play a role in the regulation of inflammation and have been linked to various autoimmune diseases, including systemic lupus erythematosus (SLE), Sjögren's syndrome, adult-onset rheumatoid arthritis (RA) and systemic sclerosis [32-34].

Interferons and their receptors

IFN are subdivided according to their association with distinct structures and interaction with cell surface receptors as type I-, type II- and type III IFN. Type I IFN constitute the largest class and comprise the well characterized members IFN-α, IFN-β, as

well as the poorly defined IFN-ε, IFN-τ, IFN-ω, IFN-δ, IFN-ζ [35]. Almost every cell is capable of producing IFN-α/β, however haematopoietic cells, particularly plasmacytoid dendritic cells produce a vast majority of IFN- α during the course of an infection [36]. Upon PAMP recognition, by the above-mentioned PRRs, type I interferon production and secretion is induced. IFN-α/β signals through the heterodimeric transmembrane type I interferon receptor (IFNAR) to regulate the expression of IFN-stimulated genes (ISGs), including Myxovirus resistance (Mx) 1 and 2, IFITM proteins, TRIM proteins, and IRFs [37], which in turn have antiviral, anti-proliferative and immunomodulatory functions. Type II IFN consists of a single member, namely IFN-γ. Its major role is the activation of macrophages, thus establishing cellular immunity by bridging the innate and adaptive immune responses [38]. Additionally, it induces the expression of genes that boost the type I IFN response [39]. IFN-γ production is mainly restricted to the cells of the immune system, especially NK cells and T cells. However, a broad range of cell types are able to respond to the cytokine. IFN-γ homodimers signal through the IFN-γ receptor complex (IFNGR1/2). Upon binding of IFNGR1, a second IFNGR1 subunit is recruited, which leads to the binding of two additional, signal-transducing IFNGR2 subunits and IFNGR complex activation and downstream signaling [38].

Type III IFNs, IFN-λ1 (IL-29), IFN-λ2 (IL-28A), IFN-λ3 (IL-28B) and IFN-λ4, are the most recently described IFNs and have similar functions as the type I IFNs [37]. However, the expression of the type III IFN receptor (IL-28Rα) is restricted to mainly epithelial cells [40]. Additionally, IFN-λ shares structural features with members of the IL-10 cytokine family and is capable to use the same low-affinity receptor subunit IL10R2 [37].

Interferon Signaling: The JAK-STAT Pathway

All interferon receptors are pre-associated with Janus kinases (JAKs) JAK1, JAK2 and TYK2, which provide the receptor with stability and control its cell surface expression (Figure 2) [37]. Type I and III IFN signaling are very similar, although they signal through different receptors. Upon binding of type I or III IFN, the receptor chains come into close proximity, allowing JAK1 and TYK2 to get activated through transphosphorylation. In turn, JAKs phosphorylate the IFN receptor chains on conserved tyrosine residues, creating binding sites for the signal transducers and activators of transcription (STAT) 1 and 2 via Src homology 2 (SH2) interaction [41, 42].

Both STATs are phosphorylated on tyrosine residues and form heterodimers, which then associate with the DNA-binding subunit IFN regulatory factor 9 (IRF9) to form the ISGF3 complex [43]. This complex translocates to the nucleus and binds to interferon-stimulated response elements (ISRE) upstream of ISGs to induce gene expression. Although ISGF3 is the predominant transcription factor in type I and III IFN signaling, other non-canonical STAT-containing complexes capable of activating ISGs have been identified in the recent years. Indeed, STAT1-independent activity has been shown to be dependent on STAT2/IRF9 during viral infection [44]. Further, STAT2/IRF9 complexes are capable to activate transcription of ISGs in a STAT1-independent manner [45-47]. In addition, an ISGF3 complex containing unphosphorylated STAT (U-STAT) has been described during the late phase of type I IFN signaling [48].

In contrast to type I and III IFN, IFN-γ signaling requires the gamma interferon-activated factor (GAF), a homodimer of phosphorylated STAT1, which translocates to the nucleus and bind to gamma-interferon activation sites (GAS), upstream of IFN-γ-induced genes [49]. In the recent years, non-canonical pathways involving STAT1/IRF9 complexes, but also $ISFG3^{II}$ complexes, containing phosphorylated STAT1, but unphosphorylated STAT2, have been described after IFN-γ signaling [50, 51]. A recent study from our lab showed that the expression of CXCL10 after IFN-γ requires STAT1 and is strongly dependent on IRF9 during DSS-induced colitis, thus reporting a non-canonical pathway of IFN-γ signaling [52].

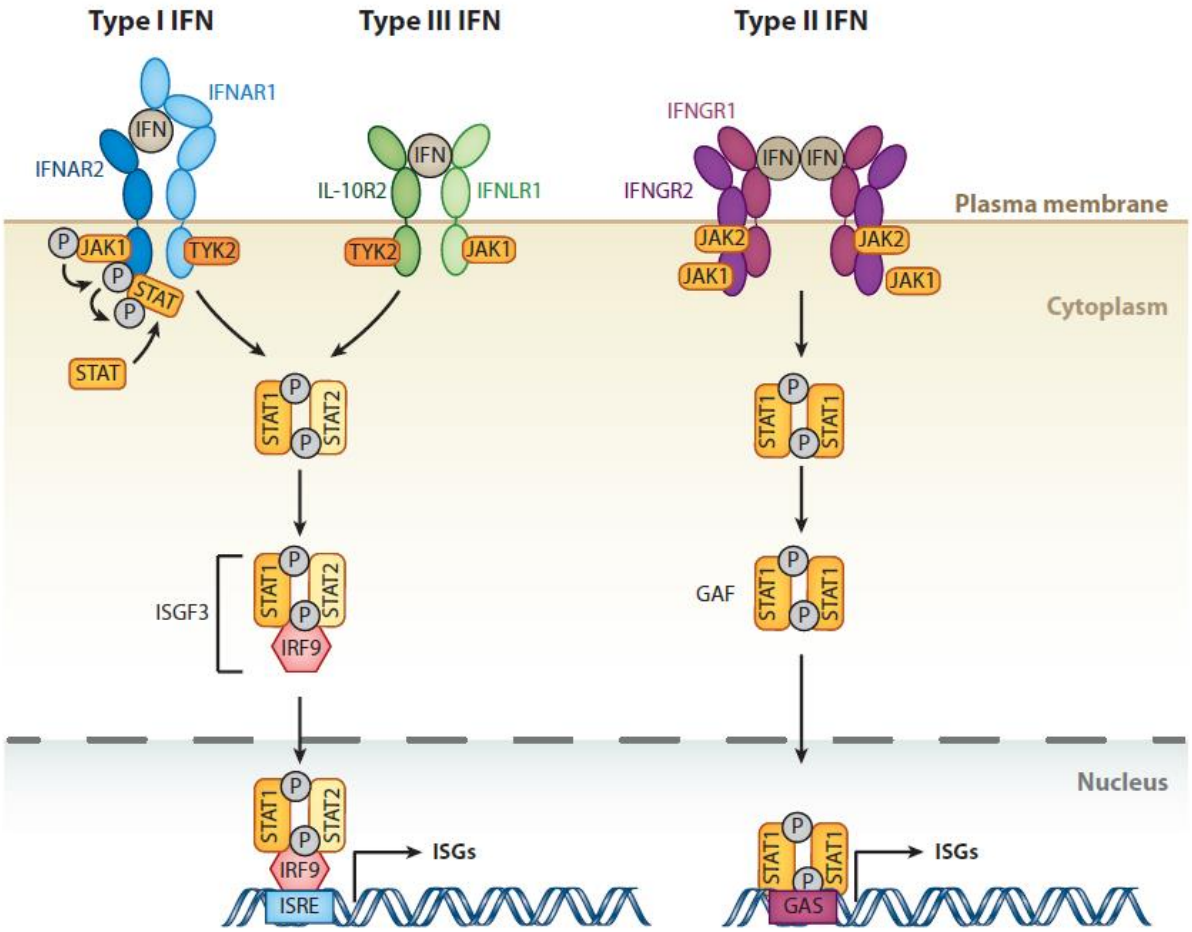

Figure 2: The interferon (IFN) signaling cascade. Three classes of IFNs signal trough different receptors complexes on the cell surface. Binding of type I and type III IFN to their respective receptors, results in the phosphorylation of the receptor-associated Janus kinase 1 (JAK1) and tyrosine kinase 2 (TYK2), which in turn phosphorylate STAT1 and STAT2. Phosphorylated STAT heterodimers associate with IRF9 to form the ISGF3 complex and translocate to the nucleus. ISGF3 binds to an ISRE site on the DNA and activates the expression of ISGs. Type II IFN signal through pre-associated JAK1 and JAK2 tyrosine kinases, leading to the phosphorylation of STAT1. STAT1 homodimers translocate to the nucleus and bind to GAS sites for the expression of ISGs. [37]

Functions of IRF9 beyond Interferon signaling

Interferon regulatory factor 9 (IRF9, also known as p48 or ISGF3γ) is best characterized as a subunit of the transcription factor ISGF3, which promotes expression of type I and III IFN-inducible genes. However, after IFN signaling several non-canonical complexes containing IRF9 have been identified and were mentioned above.

In addition to mediating innate immunity, regulatory effects of IRF9 have been linked to diseases of the heart, brain and vasculature [53].

Jiang and colleagues identified IRF9 as a negative regulator of cardiac remodelling during cardiac hypertrophy, an abnormal enlargement or thickening of the heart muscle commonly caused by high blood pressure [54]. IRF9 was shown to bind to the transcription activation domain (TAD) of myocardin, an activator of the transcription factor serum response factor (SRF), thus inhibiting its activation. This anti-hypertrophic activity of IRF9 is countered by p300-mediated activation of myocardin. Indeed, IRF9-KO mice displayed aggravated cardiac hypertrophy, whereas upregulation of IRF9 eased the symptoms.

In contrast to its protective effect in cardiac hypertrophy, IRF9 is upregulated during myocardial ischemia–reperfusion (I/R) injury, which contributes to cardiomyocyte death and inflammation through the Sirt1-p53 axis [55]. The results from Zhang et al. indicated a down-regulation of the deacetylase Sirt1 by IRF9, which promotes the corresponding apoptotic signaling through p53, thus contributing to I/R-induced cardiomyocyte death.

Similarly, IRF9 was also described to decrease Sirt1 activity, hence p53 acetylation, leading to cell death signaling in neurons in context of a cerebral ischemic stroke [56]. In the past, IRF9 and other members of the IRF family, such as IRF2, have also been shown to physically interact with the p65 subunit of NFκB in neural cells. However, the effect of this interaction on stroke remains enigmatic [57].

The IRF9/Sirt1 axis has also been described as a vascular injury response pathway that promotes vascular smooth muscle cell (VSMC) proliferation in the context of neointima formation, a scar tissue that forms in blood vessels, following vascular injury [58].

Unrelated to cardiovascular diseases, IRF9 was reported to have a protective role in metabolic disorders. It was shown to bind to peroxisome proliferator-activated receptor α (PPARα) to activate target gene expression in the liver, mostly involved in lipid metabolism, thus attenuating insulin resistance and steatosis hepatis (fatty liver) in obese mice [59].

Together, these findings indicate that IRF9 not only acts as a transcription factor, but also cooperates with other transcription factors in order to regulate downstream gene expression.

The NFκB pathway

The NFκB transcription factor family consists of five related proteins, namely p65 (RelA), RelB, c-Rel, p105/p50 and p100/p52. All the members of this family share a conserved 300 amino acid long Rel homology domain (RHD) at the amino-terminus, required for dimerization, IκB interactions and DNA binding to target DNA sequences called κB sites. Additional protein domains mediate the recruitment of co-activators and co-repressors to regulate target gene expression [60, 61]. p65, RelB and c-Rel possess a transactivation domain (TAD) allowing them to initiate transcription through recruitment of transcriptional co-activators. However, p50 and p52 do not have any TAD and must therefore form heterodimers with p65, RelB or c-Rel to activate transcription. The NFκB family plays an important role in the induction of inflammatory genes during infection. Different signaling routes lead to the activation of NFκB, which can be classified into canonical and non-canonical pathways. However, for this thesis we will only focus on the canonical pathway, among which the best-characterized inducers are the PRR and members of the TNF family of cytokines [61].

Canonical NFκB consists of two subunits, p50 and p65, and is associated with inhibitor of κB (IκB) in unstimulated cells. This association masks the nuclear translocation signal (NLS) of NFκB, thus preventing it from shuttling to the nucleus and initiating transcription. Upon PRR stimulation, the IκB kinase (IKK) complex, consisting of two catalytically active kinases IKKα and IKKβ and a regulatory scaffold protein NEMO (IKKγ), is activated triggering a phosphorylation-induced proteasomal degradation of IκB-α [62]. In turn, NFκB is post translationally modified, including the phosphorylation of p65 at Ser276 and acetylation of Lys310 [63], triggering its translocation to the nucleus in order to bind target promotors and induce expression of proinflamatory genes, such as TNFα, IL-1, IL-6 and IL-12 [64]. Additionally, NFκB drives the expression of IκB-α, generating a negative feedback loop for its regulation.

Other than regulating inflammation responses during infection, NFκB is involved in a myriad of activities, including the development and maturation of innate and adaptive immune cells [60]. Further, deregulation of the NFκB can result in a variety of diseases including cancer, chronic inflammation- and autoimmune diseases [65].

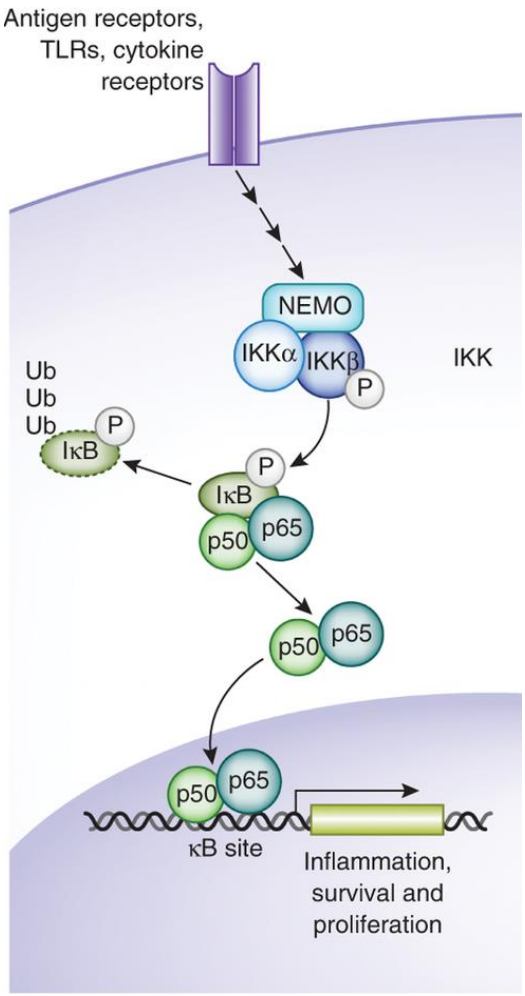

Figure 3: The canonical NFκB signaling pathway. Signaling by PRR and cytokine receptors, including the TNF receptor, activates the IKK complex composed of IKKα, IKKβ and NEMO (IKKγ), leading to the phosphorylation of IκB. IκB phosphorylation is followed by ubiquitination and proteasome-induced degradation. This allows NFκB to translocate to the nucleus and to bind to specific DNA sequences (κB sites), inducing the transcription of inflammatory genes. [66]

The machinery of transcriptional activation

The enzyme responsible for the transcription of DNA into RNA is the RNA polymerase (Pol). In eukaryotes three different RNA polymerases (I, II and III) are known and are required for the synthesis of different types of RNAs. RNA Pol II, together with the mediator complex and a large number of transcription factors is responsible for the synthesis of mRNA of protein-coding genes. The RNA Pol II consists of 10 subunits in yeast and 12 in humans. Rbp1, the biggest subunit of Pol II contains a carboxy-terminal domain (CTD) with 25-52 heptarepeats (Tyr1 Ser2 Pro3 Thr4 Ser5 Pro6 Ser7), depending on the species [67]. The CTD is subject to many modifications, which regulate the Pol II activity. It functions as a binding scaffold for a variety of nuclear factors [68]. The most prominent and well-characterized modification is the

phosphorylation at the serine residues 2, 5 and 7. Nevertheless, glycosylation, ubiquitination and methylation have also been reported [69]. Different kinases are required for the phosphorylation of these relevant serine residues within the heptarepeat. Pol II with a hypophosphorylated CTD is initially recruited to the promoter during pre-initiation complex (PIC) formation and is phosphorylated at Ser5 during transcription initiation by CDK7, the kinase subunit of the general transcription factor TFIIH [70, 71]. During initiation, only a short stretch of DNA is transcribed, followed by a pause, which is caused by an elongation block by the DSIF and NELF proteins [72, 73]. This process is referred to as “promoter clearance” and is important for the proper synthesis of the methylguanosine cap at the 5’end of the mRNA, the association of the splicing machinery and histone-modifying enzymes with the Pol II CTD [74]. Next, the Pol II proceeds with the elongation of the mRNA, which requires a phosphorylation of Ser2 by CDK9, the kinase subunit of the elongation factor pTEFb. In addition, DISF and NELF need to be phosphorylated by CDK9 in order to release the elongation block [70, 71]. As elongation continues, Ser2 phosphorylation (Ser2P) increases, while Ser5 phosphorylation (Ser5P) is progressively removed by phosphatases. Indeed, Ser5P peaks around the transcription start (TSS), whereas Ser2P accumulates towards the end of the gene [71].

Although Ser2P and Ser5P have been well characterized, CDK7 has also appeared to phosphorylate Ser7 [75], whereas CDK9 is required for Thr4 phosphorylation [76]. However, the role of these modification in the transcription of protein-coding genes have not been fully understood. Ser7 phosphorylation (Ser7P) is thought to play a role in the transcription of snRNA [77] and a range of protein-coding genes, displaying a gene-specific feature of Ser7P [71]. ChIP analysis indicates that phosphorylated Ser7 is mostly found at the 3’end of protein-coding gene, suggesting a role in transcriptional termination or 3’end processing [78].

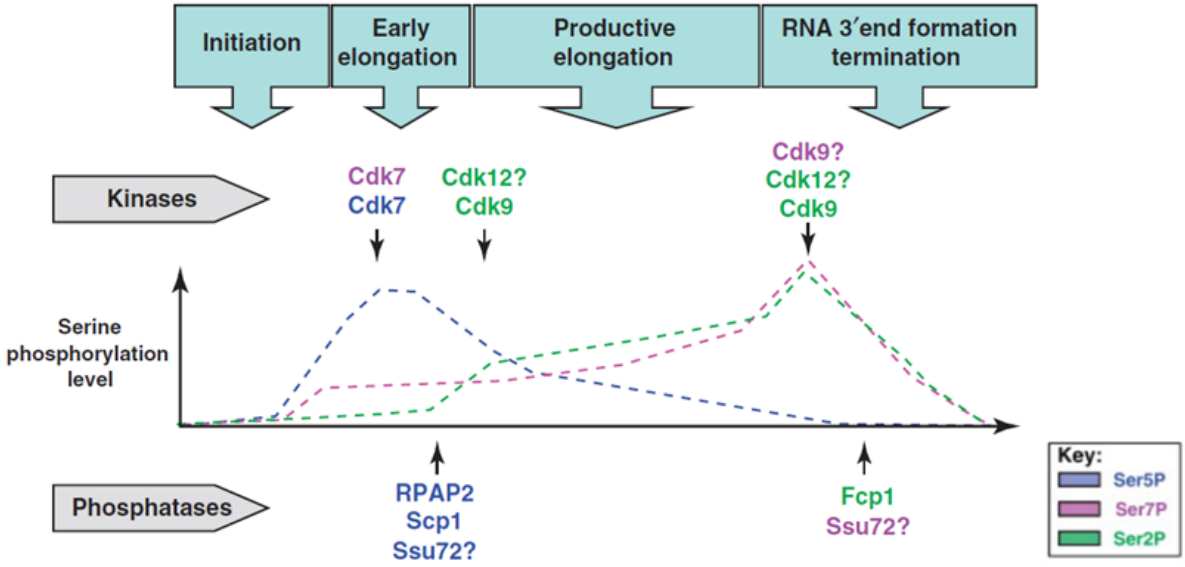

Figure 4: The carboxyl-terminal domain (CTD) phosphorylation pattern. Average level of Ser2, Ser5 and Ser7 phosphorylation, detected on protein-coding genes during the different steps of the transcription cycle is represented in this figure. [78]

Regulation of Nos2 gene by STAT and NFκB transcription factors during infection with *Listeria monocytogenes*

Listeria monocytogenes

Listeria monocytogenes is a facultative intracellular Gram-positive bacterium and the causative agent of listeriosis, when ingested with contaminated food. Although healthy people are at low risk, *L. monocytogenes* infection can cause lethal complications in immunocompromised individuals and abortions in pregnant women through the ability of the bacterium to cross the placental barrier [79, 80]. *L. monocytogenes* encodes 10 virulence genes that contribute to bacterial invasion, cytosolic entry and growth, intracellular motility and spread to adjacent cells. These genes are regulated by the transcription factor PrfA, whose expression is under control of an RNA thermosensor. After invading the host through the gastrointestinal tract, PrfA becomes activated due to the temperature increase, which leads to gene expression [81]. As the first line of defence macrophages engulf bacteria and are the prominent host of *L. monocytogenes*. *L. monocytogenes* has the ability to escape the phagosome into the cytoplasm, where it replicates and uses the host cell actin system to move within the cytoplasm and for cell-to-cell spread [82]. Hence, *L. monocytogenes* is recognized by both extracellular and cytoplasmic PRRs within the host cell. As soon as *L. monocytogenes* is recognized by TLR, the transcription factor NFκB is activated, leading to the expression of proinflammatory cytokines. Recognition of *L. monocytogenes* in the

cytoplasm by different cytosolic sensors activates IRF3 through its phosphorylation and induces the expression and secretion of type I interferons, leading to the expression of interferon-stimulated genes (ISGs) [83, 84].

It is possible to separate these pathways *in vitro* by stimulating the cells on one hand with heat-killed *Listeria* (hkL), leading only to the activation of NFκB and on the other hand by treating cells with recombinant IFN-β, triggering the formation of the ISGF3 complex.

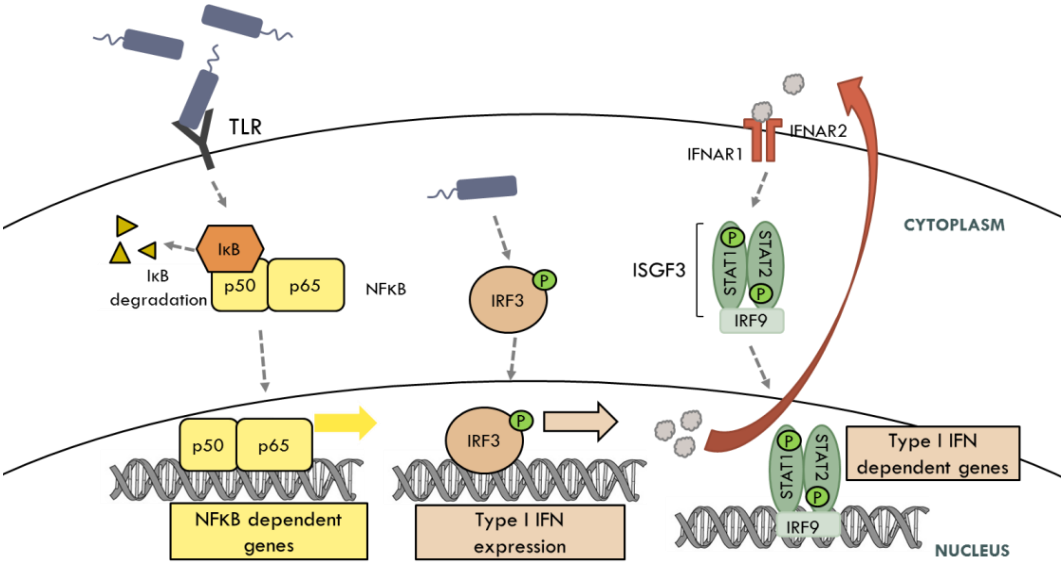

Figure 5: Recognition of *L. monocytogenes* in macrophages and activation of signaling pathways. *L. monocytogenes* is first sensed by PRR at the cell surface, leading to the phosphorylation-induced proteosomal degradation of IκB and translocation of NFκB to the nucleus, resulting in the expression of pro-inflammatory genes. Because of its ability to evade the phagosome, *L. monocytogenes* is also recognized in the cytoplasma, triggering IRF3 phosphorylation and the expression of type I IFNs. In turn IFNs activate the expression of ISGs though the JAK/STAT signaling pathway. [Figure by Ekaterini Platanitis]

Inducible nitric oxide synthase (iNOS)

The *Nos2* gene, encoding the inducible nitric oxide synthase (iNOS), is an enzyme catalysing the formation of NO radicals from the conversion of arginine to citrullin. In contrast to other NO synthases, *Nos2* expression is undetectable in resting cells, but highly induced during infection. NO is primarily considered as an antimicrobial agent, but has also been shown to affect cell survival and to exert anti-tumour activity [85-87]. In the case of *Listeria monocytogenes* infection, the role of NO is not clear, since

controversial studies showed that NO can either be harmful or beneficial during *L. monocytogenes* infection [88-90].

Nos2 expression is regulated by IFN-γ through IRF1 and STAT1 homodimers, since ablation of one of these genes results in a diminished production of NO in macrophages [91, 92]. However, inducibility of *Nos2* by IFN-γ alone is quite weak compared to the synergistic activity of IFN-γ together with the TLR agonist LPS [93]. After treatment of macrophages with LPS alone or in *L. monocytogenes*-infected macrophages, *Nos2* and the synthesis of type I IFNs are strongly induced. Additional studies emphasise the importance of type I IFNs for *Nos2* expression [94, 95]. On the other hand, type I IFNs alone were poor inducers of *Nos2* expression, suggesting the importance of another pathway cooperating with the activity of the type I IFN receptor.

NFκB-ISGF3 cooperativity in *Nos2* regulation

Studies in our lab have shown that unlike classical IFN-I-stimulated genes (ISGs) or NFκB target genes, full-blown transcriptional activation of the *Nos2* gene during infection with *Listeria monocytogenes* requires coordinate assembly of an initiation complex by the transcription factors NFκB and type I interferon-activated ISGF3 [96]. Indeed, NFκB binding to the *Nos2* promoter occurred after exposure of bone marrow-derived macrophages to hkL, whereas ISGF3 binding was caused by treatment with recombinant IFN-I. In turn, these transcription factors are responsible for the recruitment of several factors of the transcriptional machinery. First, TFIIH and its kinase subunit CDK7 are recruited by NFκB to the *Nos2* promoter [96]. Additionally BET proteins, especially Brd4 play a role by stabilizing THIIF/CDK7 binding to the promoter even after NFκB has left the DNA [97]. MLL1-2 COMPASS H3K4 methyl transferase complex and CBP histone acetyl transferase (HAT) enrichment is similarly NFκB-dependent, which is thought to produce transcription-friendly chromatin [98]. Furthermore, NFκB is responsible for the recruitment of the mediator kinase module CDK8. The mediator is a multi-protein complex composed of 26 subunits in mammals and evolutionary conserved among eukaryotes. The role of the mediator complex is to regulate the Pol II and to mediate contacts between transcription factors and the machinery of transcription, communicating regulatory signals from DNA-bound transcription factors to the Pol II enzyme. The kinase module CDK8 is required for

pTEFb/CDK9 association with the *Nos2* promoter. Indeed, CDK9 and CDK8 have been co-immunoprecipitated from BMDM lysates [98].

At a later stage, ISGF3 binds to the DNA, which is necessary for the formation of the pre-initiation complex (PIC), in particular the binding of TFIID. In addition, ISGF3 contributes to the recruitment of the mediator core, as well as Pol II recruitment. As soon as Pol II joins the transcriptional machinery, Ser5 and Ser2 on its CTD are phosphorylated by CDK7 and CDK9, respectively, to initiate transcription [96-98]. In short, NFκB and ISGF3 work together for the recruitment of the mediator complex and the completion of the transcriptional machinery at the *Nos2* promoter. *Nos2* is not the sole example of a gene being coregulated by both NFκB and ISGF3. In total, 127 genes that were synergistically induced by hkL/NFκB and IFN-I/ISGF3 have been identified, including *Il6*, *Ccrl2* and *Il1m* [98]. The mechanism of transcription cooperativity shown for *Nos2* has also been confirmed for *Il6*.

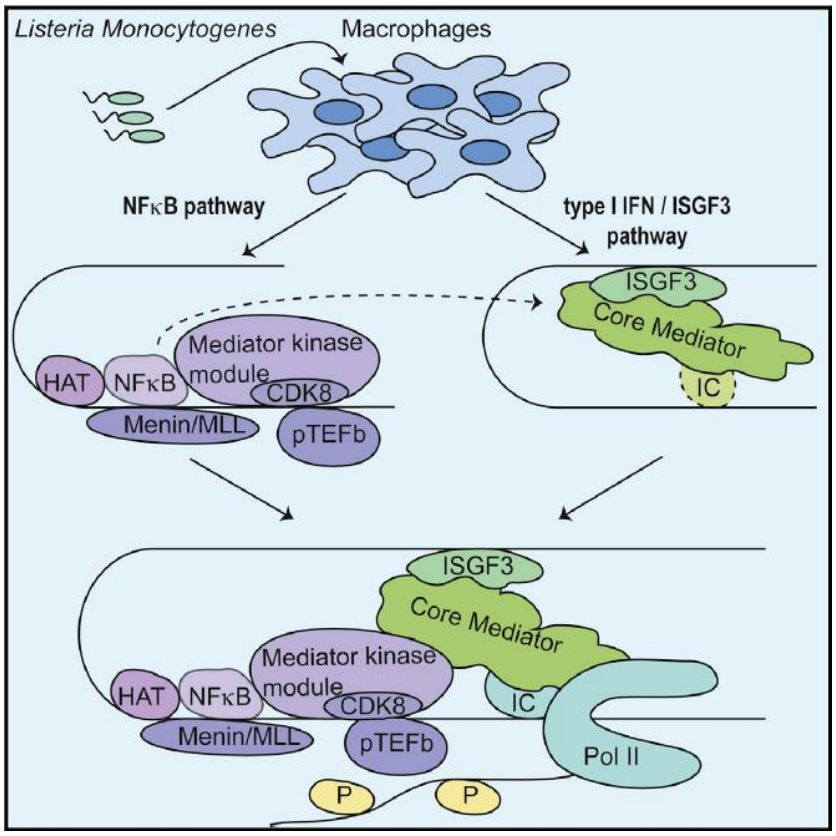

Figure 6: Cooperative assembly of the transcriptional machinery at the *Nos2* promoter in *L. monocytogenes*-infected macrophages. NFκB recruits histone-modifying enzymes, the mediator kinase module, including CDK8, the transcription factor TFIIH/CDK7 and pTEFb/CDK9 to the *Nos2* promoter. On the other hand, ISGF3 is essential for the binding of the pre-initiation complex, the core mediator, as well as the RNA polymerase II. [98]

Aims

The goal of this thesis was to examine three major topics.

A previous study of our lab has shown that simultaneous addition of hkL and IFN-β to bone marrow-derived macrophages (BMDM) mimics the ability of an infection with *L. monocytogenes* to cause high levels of iNOS mRNA expression [96]. Since both infection and hkL stimulate production of TNF, we wondered to which extent TNF contributed to NFκB activation and iNOS induction.

The aim of the second part of this thesis was to determine if the NFκB-dependent recruitment of CDK7 to the *Nos2* promotor is a result of a direct interaction between the p65/RelA subunit and the CDK7 serine 5 kinase. A previous study in our lab [96] proposes an NFκB-dependent recruitment of the TFIIH/CDK7 complex, providing a Ser5 kinase activity for the Pol II CTD. However, how exactly TFIIH/CDK7 is recruited, remains unknown.

The third part of this thesis, dealt with the generation of an IRF9-specific monoclonal antibody, since no murine IRF9 antibody, that is suitable for western blot and chromatin immunoprecipitation, is commercially available. This project was in collaboration with Egon Ogris' lab (Max F. Perutz Laboratories). My part of the project consisted in the generation of a bacterial expression plasmid containing murine IRF9, the expression of the protein in *E. coli* and its purification. Furthermore the antibody's function had to be verified in context of ChIP and IP experiments.

This antibody would provide a valuable tool for further analysis of IRF9-dependent genes via ChIP-seq, since one of our recent studies proposes an important role for IRF9 as a component of non-canonical Stat complexes in the development of colitis [52].

Materials and Methods

Mice and Cells

Wt C57BL/6 and IRF9−/− mice [99] were sacrificed between 6 and 12 weeks of age for bone marrow isolation. Skin and muscles were removed from the hind legs and tibiae and femurs were collected in PBS. The tips of the bones were cut and DMEM (+ 10% L929 cell-derived colony stimulating factor 1 mixture + 10% FCS + Pen/Strep) was flushed through the bones with a syringe. Cells were collected in a falcon tube and plated on 10 cm square dishes. After 3-4 days, fresh LCCM (L Cell Conditioned Medium) was added to the cells. When they reached confluency, the cells were split at a ratio of 1:2 or 1:3. After 9-12 days, differentiated bone marrow-derived macrophages (BMDM) were used for experiments [100]. If a higher cell number was necessary, additional macrophage colony stimulating factor (M-CSF) was added to the medium.

RAW 264.7 macrophages, human embryonic kidney 293 (HEK293) cells [101], Wt and IRF9−/− mouse embryonic fibroblasts (MEF) were cultured in DMEM (10% FCS, 1x Pen/Strep) at 37°C, 5% CO_2.

Reagents

Recombinant IFN-γ (eBioscoence) was added to the culture medium to a final concentration of 10 ng/ml.

Cells were treated with 250 U/ml recombinant IFN-β (pbl Assay Science) for 2h.

Heat-killed Listeria (hkL), generated by incubation of an overnight culture at 70 °C for 20 minutes, was added to the culture medium at a multiplicity of infection (MOI) of 50.

TNF-α was used at a concentration of 20 ng/µl.

Cloning

Cloning genes into bacterial and mammalian expression vectors

The coding region of several murine genes was cloned into bacterial and mammalian expression plasmids, namely pGEX4T-1 (GE Healthcare Life Sciences), pET23a+ (Novagen), pET-Duet1 (Novagen) and pCMV (Clontech) (Table 1).The genes were amplified by PCR (95 °C for 2 min, 25× (95 °C for 15 sec, 60 °C for 15 sec, 72 °C for 15 sec), 95 °C for 15 sec) from primary bone marrow-derived macrophage (BMDM) cDNA using Q5 polymerase (New England Biolabs Inc.).The sequence of the primers

used for the amplification of the genes of interest can be found in the appendix. Both vectors and inserts were respectively digested by the same restriction enzymes (FastDigest, Thermo Scientific). The vector was incubated for 10 min with alkaline phosphatase (FastDigest, Thermo Scientific to avoid its religation by removing the phosphate groups at the 5' ends. Ligation was performed with the T4 Ligase (Thermo Scientific) at 22 °C for 1h. Plasmids containing a gene of interest were transformed into *Escherichia coli* TOP10 strain by heat-shock. Plasmid DNA was purified using the QIAGEN MiniPrep Kit and sent for sequencing to LGC Genomics (Berlin, Germany).

Gene	Species	Tag	Terminus	Plasmid	Expression System	Resistance	Restriction Enzymes [fw/rv]
p65/RelA	mouse	GST	N	pGEX4T1	bacterial	Amp	EcoRI/XhoI
p65/RelA	mouse	myc	N	pCMV	mammalian	Amp	EcoRI/XhoI
p65/RelA	mouse	HA	N	pCMV	mammalian	Amp	EcoRI/XhoI
p50	mouse	myc	N	pCMV	mammalian	Amp	EcoRI/XhoI
p50	mouse	HA	N	pCMV	mammalian	Amp	EcoRI/XhoI
IRF9	mouse	6 His	N	pETDuet1	bacterial	Amp	EcoRI/HindIII
IRF9	mouse	6 His	C	pET23a+	bacterial	Amp	NheI/XhoI
IRF9	mouse	myc	N	pCMV	mammalian	Amp	EcoRI/XhoI
IRF9	mouse	HA	N	pCMV	mammalian	Amp	EcoRI/XhoI
Cyclin H	mouse	myc	N	pCMV	mammalian	Amp	XhoI/NotI
Cyclin H	mouse	HA	N	pCMV	mammalian	Amp	XhoI/NotI
CDK7	mouse	GST	N	pGEX4T1	bacterial	Amp	BamHI/EcoRI
CDK7	mouse	6 myc	N	N-6myc	mammalian	Amp	Gateway

Table 1: Generated bacterial and mammalian expression plasmids.

Cloning CDK7 using Gateway technology (Invitrogen)

The coding region of murine CDK7 was amplified by PCR (95 °C for 2 min, 25× (95 °C for 15 sec, 60 °C for 15 sec, 72 °C for 15 sec), 95 °C for 15 sec) from BMDM cDNA using Q5 polymerase (New England Biolabs Inc.) and primers, suitable for gateway cloning (appendix). A 100 fM equimolar solution of the PCR product and the donor vector were incubated for 1h at 25°C with the Gateway B Clonase II Enzyme Mix to allow the BP recombination. The reaction was stopped by addition of 2 µl proteinase K and 10 minutes incubation at 37°C. The entry vector was then transformed and propagated in TOP10 *E. coli* strain. For the LR recombination, 300 ng of both

entry and destination vectors were incubated with the LR Clonase Enzyme Mix for 1 h at 25 °C. The reaction was stopped by addition of 2 µl proteinase K and 10 minutes incubation at 37°C. The destination vector now containing the coding sequence of murine CDK7 and an N-terminal 6× myc-tag was then transformed into TOP10 *E. coli*. Because of the lethal effects of the CcdB protein, which is found in the donor and destination vector, this vector must be propagated in an E. coli strain that is resistant to CcdB effects. Although the E. coli TOP10 strain is not advertised of being resistant to CcdB, donor and destination vectors could be propagated in this strain.

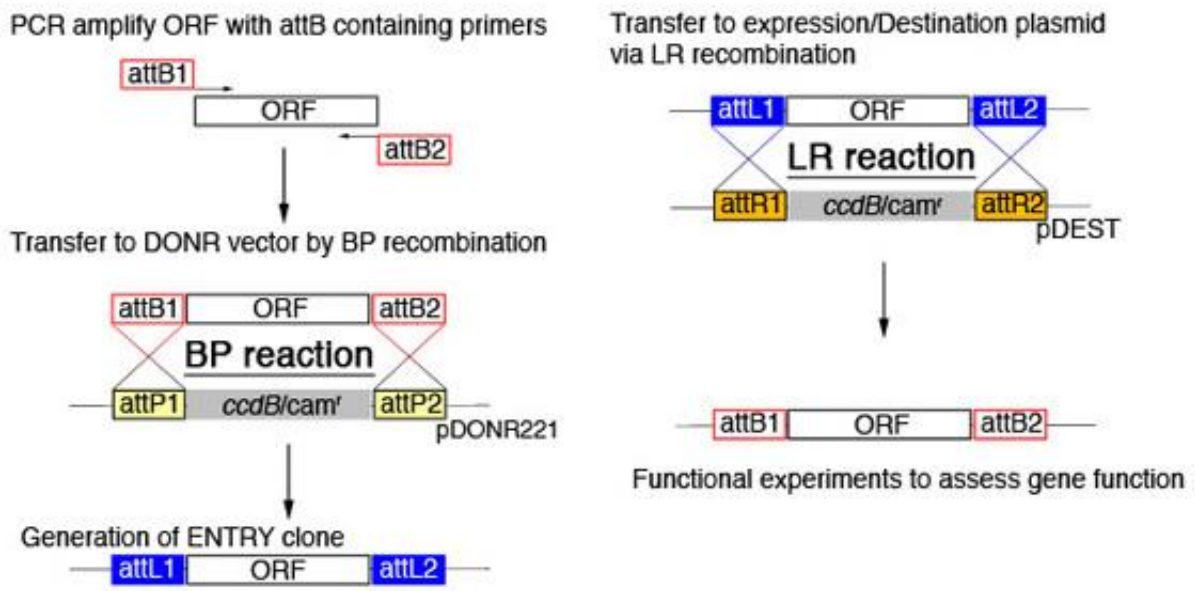

Figure 7: Schematic of the Gateway cloning technology (Invitrogen). (Figure by Lawson Laboratory, Gateway cloning overview)

Purification of Plasmids

Plasmid DNA was purified using the Qiagen Maxi Kit (Cat.No. 12163) and following the manufacturer's protocol, optimized by the Versteeg group.

A colony was picked from the agar plate and inoculated in 2 ml LB medium, containing selective antibiotics at 37 °C for few hours in order to grow a starter culture. From this, 400 ml LB medium containing selective antibiotic are inoculated 1:500-1:1000 and cultured over night at 37 °C. The next morning, 500 µl of the bacterial culture were mixed 1:1 with glycerol and stored at -80 °C. The remaining volume was centrifuged for 10 minutes at 10000 ×g and the bacterial pellet was resuspended in 10 ml P1 buffer. Bacteria were lysed by the addition of 10 ml P2 buffer containing RNaseA and inverted 5-6 times. Thereafter, 10 ml of the neutralisation buffer P3 was added and the liquid was inverted 7-8 times and incubated on ice for 10 minutes. Centrifu-

gation for 30 minutes at 10000 ×g at 4 °C pellets the white precipitate that has formed after neutralization, the maxi prep columns were equilibrated with QBT buffer. The plasmid DNA was bound to the column, abundantly washed with QC buffer and then eluted with 15 ml QF elution buffer into 10.5 ml absolute isopropanol. The tubes were then centrifuged for 30 minutes at 3220 ×g at 4 °C. The DNA pellet was washed twice in 70 % Ethanol and dried, before being dissolved in 500-1000µl nuclease-free water at 65 °C for 20 minutes. The DNA concentration was measured with NanoDrop.

Transformation of Plasmid DNA in different *E. coli* strains

About 50-100 ng plasmid DNA was added to 50 µl of different competent *E. coli* strains, such as TOP10, DH5α, Rosetta pLysS and SoluBL21. Bacteria were heat-shocked for 45-60 seconds at 42 °C, then cooled on ice. Next, bacteria were plated on 1 % LB-agar plates, containing selective antibiotic.

Expression and Isolation of Fusion Proteins in *E. coli*

The bacterial expression plasmids containing the GST- or 6xHis-tagged proteins were transformed into *Escherichia coli* Rosetta pLysS, a strain in which protein expression can be induced by isopropyl β-D-thiogalactoside (IPTG) (Invitrogen). The cultures were grown in LB medium to an OD_{600} of 0.5 or 0.8. Protein expression was then induced by addition of 0.1-1.0 mM IPTG to induce protein expression either over night at 18 °C or at 37°C for 4 h. Cells were harvested by centrifugation (15 min, 4000 ×g) and lysed in the appropriate lysis buffer depending on the tag of the fusion protein.

Isolation of GST-tagged proteins

For the isolation of GST-tagged proteins, bacteria were lysed in lysis buffer (125 mM Tris HCl pH 7.4, 300 mM NaCl, 1% v/v Tween 20, protease inhibitors (Roche Life Sciences), DNase I (New England Biolabs Inc.), 1 mM DDT) for 30 min at 4 °C. GST-tagged proteins were pulled down with Pierce Glutathione Magnetic Beads (Thermo Scientific) and eluted in lysis buffer containing 50 mM reduced glutathione (125 mM Tris HCl pH 7.4, 300 mM NaCl, 0.05 % v/v Tween 20). Complete lysate, soluble protein fraction and eluted proteins were analysed by using 12% SDS-polyacrylamide gels and by Coomassie Blue staining (Coomassie brilliant blue R, 2-Propanol, 10% Acetic Acid).

Isolation of soluble 6×His-tagged proteins

For the isolation of His-tagged proteins, pelleted bacteria were lysed in lysis buffer (50 mM NaH_2PO_4 pH 7.5, 300 mM NaCl and 10 mM imidazole (peqlab), protease inhibitors (Roche Life Sciences), DNase I (New England Biolabs Inc.) for 30 min at room temperature. After clearing the lysate by centrifugation at 14000×g for 10 minutes, soluble His-tagged proteins were pulled down with equilibrated Ni Sepharose 6 Fast Flow beads (GE Healthcare) for 2h at 4°C, washed 3 times with lysis buffer containing 50 mM imidazole and eluted in lysis buffer containing 250 mM imidazole. Complete lysate, soluble protein fraction and eluted proteins were analysed in 12% SDS-polyacrylamide gels and stained by Coomassie Blue staining (Coomassie brilliant blue R, 2-Propanol, 10% Acetic Acid).

Isolation of insoluble His-tagged proteins

For the isolation of insoluble His-tagged proteins, the pellet from the cleared lysate, was resuspended in buffer A (6 M Guanidinium HCl, 100 mM NaH_2PO_4 and 10 mM Tris HCl pH 8.0) and incubated for 30 minutes at room temperature with periodical vortexing. In the meantime, the Ni Sepharose 6 Fast Flow beads (GE Healthcare) were equilibrated with buffer A. Hereafter, the samples were cleared by centrifugation for 10 minutes at 14000×g. The supernatant was mixed with the Sepharose beads and incubated for 2h at room temperature on a rotator, washed 3 times with lysis buffer containing 50 mM imidazole and eluted in lysis buffer containing 250 mM imidazole. After each step, the samples were centrifuged for 5 minutes at 600 ×g to sediment the sepharose beads. The eluate containing the insoluble fraction of His-tagged proteins was analysed alongside the soluble fractions of His-tagged proteins.

Transfection of HEK293 and MEFs

When seeded into 6-well plates, 1.5-2.0 $x10^6$ HEK293 cells per well or 1.2-1.8 $x10^5$ mouse embryonic fibroblasts (MEF) per well were used for transfection, whereas 6.0-6.5 $x10^6$ HEK293 cells or 1.2-2.0 $x10^6$ MEFs were seeded in a 10 cm plate. The next day, 2-5 µg of mammalian expression plasmids DNA, diluted in 200 µl DMEM and 8-12 µl Turbofect (Thermo Scientific) were incubated for 20 minutes at room temperature and added dropwise to the culture medium. The next day, cells were washed twice in cold PBS and lysed in an appropriate lysis buffer, depending on the further application. For western blot detection of transfected protein, the cells were lysed in Laemmli buffer (120 mM Tris HCl pH 8, 2% SDS, 10% glycerol) and boiled at 95 °C

for 10 minutes. For immunoprecipitation, the cells were either lysed in Frackelton buffer (10 mM Tris, 50mM NaCl, 30 mM NaPPi, 50 mM NaF, 1% Triton X-100, pH 7-7,5, complete EDTA-free protease inhibitor cocktail (Sigma Aldrich), 1 mM PMSF, 100 µM sodium orthovanadate, 1 mM DTT), RIPA buffer (50 mM Tris HCl pH 8, 150 mM NaCl, 1% NP-40, 0.5% sodium deoxycholate, 1 mM DTT, 1 mM PMSF, 1 mM Sodium orthovanadate and complete EDTA-free protease inhibitor cocktail (Sigma Aldrich) or a non-denaturing lysis buffer (20 mMTris HCl pH 8, 137 mM, NaCl, 1% NP-40, 2 mM EDTA). However, for RNA isolation the cells were lysed in Buffer RA1 + 1:100 β-mercaptoethanol according to the manufacturer's instructions (Machery-Nagel).

Protein Extraction

For western blot analysis, cells were washed twice with cold PBS and scraped in Laemmli buffer (120 mM Tris HCl pH 8, 2% SDS, 10% glycerol) for lysis. The lysates were then boiled for 10 minutes at 95 °C. An aliquot was mixed with β-mercaptoethanol and bromophenol blue and loaded on an SDS polyacrylamide gel.

RNA isolation

Cells were washed twice with cold PBS and kept on ice, before starting the RNA isolation using the Total RNA Isolation Kit (Macherey-Nagel) and following the manufacturer's instructions.

cDNA Synthesis

For cDNA synthesis, 400 ng RNA were dissolved in nuclease free water. 1 pmol oligo dT18 was added the samples and were incubated for 5 minutes at 70°C. Next, the samples were cooled down on ice and RT buffer, 1 mM dNTPs and nuclease-free water were added to each sample and incubated for 5 minutes at 37°C. 200 U reverse transcriptase was added and samples were incubated for 1h at 42°C (RevertAid Reverse Transcriptase (200 U/µL), Life Technologies). To stop the reaction, samples were incubated for 10 minutes at 70°C and diluted 1:10 in nuclease free water.

Quantitative real-time PCR

Quantitative RT-PCR using an Eppendorf Realplex mastercycler 2, was performed by using the polymerase GoTaq qPCR Mastermix (Ref: A600A, Promega, USA). The

PCR program was the following: 95 °C for 2 min, 35× (95 °C for 15 sec, 60 °C for 15 sec, 72 °C for 15 sec), 95 °C for 15 sec, from 60 °C to 95 °C in 20 min for the melting curve, 60 °C for 2 min. Primers for the Nos2, IL-6, IκB-α, Mx1, Mx2 and GAPDH genes were used (appendix). Fold induction was calculated by normalizing to the GAPDH housekeeping gene and to the untreated sample.

Determination of protein concentration via Pierce BSA Protein Assay

A BSA standard solution of 0, 0.25, 0.5, 0.75, 1, 1.5, 2 mg/ml was prepared. Protein samples were heated for 5-10 minutes at 95°C. 5 µl of each standard solution and 5 µl of each sample were diluted 1:10 in a 96-well plate. 200 µl of a 1:50 solution of reagent “A” + reagent “B” were added. The plate was then incubated for 15-20 minutes at 37°C. To determine the protein concentration the OD was measured at 595 nm. Using the BSA standard, a calibration curve was calculated and sample concentration was determined.

Immunoprecipitation (IP)

$6.5x10^6$ HEK293 cells were seeded in a 10 cm plate and transfected with mammalian expression plasmids using Turbofect (Fermentas). Approximatively 16 hours post-transfection, the cells were washed twice in cold PBS and lysed in RIPA buffer (50 mM Tris HCL pH 8, 150 mM NaCl, 1% NP-40, 0.5% sodium deoxycholate, 1 mM DTT, 1 mM PMSF, 1 mM Sodium orthovanadate and cOmplete EDTA-free protease inhibitor cocktail (Sigma Aldrich)) for 1-2 h at 4 °C. The lysates were centrifuged for 5 minutes at 14000×g and precleared with magnetic Dynabeads Protein G (Life Technologies) for 1h at 4 °C to reduce non-specific binding of proteins to the magnetic beads.

Crosslinking IgGs to Dynabeads Protein G

The Antibody-coupled Dynabeads Protein G were washed twice in Conjugation buffer (20 mM sodium phosphate, 150 mM NaCl) before being resuspended in conjugation buffer containing 5 mM Bissulfosuccinimidyl suberate (BS^3) (Thermo Scientific) and incubated for 1h at room temperature on a rotator. The reaction was quenched after addition of quenching buffer (1 M Tris HCl pH 7.5) and 25 minutes of incubation with rotation. The cross-linked beads were washed three times with RIPA buffer and used for immunoprecipitation.

Co-Immunoprecipitation of overexpressed fusion proteins

50 µl of magnetic beads per sample, were incubated with myc-tag, HA-tag or p65 specific antibodies (appendix) for 2-3 h at 4 °C and cross-linked, using (BS^{3}) (Thermo Scientific). The magnetic beads were previously blocked in RIPA buffer, containing 5 % BSA for 1 h at 4°C. Hereafter, the cross-linked beads were incubated with the lysates, containing 1 mg proteins, overnight at 4 °C on a rotator. The next day, the beads were washed three times with RIPA buffer and proteins were eluted by boiling the beads at 95 °C for 10 minutes in SDS sample buffer (250 mM Tris-HCl pH 6.8, 20% Glycerol, 1.6% SDS, 20% β-Mercaptoethanol, 0.002% Bromophenol blue).

IRF9 with hybridoma supernatants

After clearing the lysates, 1 mg protein was adjusted to a volume of 900 µl and incubated over night at 4 °C on a rotator with 100 µl of hybridoma culture supernatant, containing secreted IRF9 specific antibodies. 50 µl magnetic beads per sample were blocked in RIPA buffer, containing 5 % BSA over night at 4°C. The next day, the beads were incubated with the lysate-antibody mix for 3-4 hours at 4 °C and washed three times with RIPA buffer. Proteins were eluted by boiling the beads at 95 °C for 10 minutes in SDS sample buffer (250 mM Tris-HCl pH 6.8, 20% Glycerol, 1.6% SDS, 20% β-Mercaptoethanol, 0.002% Bromophenol blue).

Chromatin Immunoprecipitation (ChIP)

1.5 $\times 10^{7}$ BMDMs were seeded in a 15 cm dish and treated with 10 ng/ml IFN-γ and 250 U/ml IFN-β for the indicated period. Proteins and DNA were crosslinked with 1 % formaldehyde for 10 minutes at RT and the reaction was stopped by adding 125 mM glycine for 10 minutes. The cells were washed and scraped in cold PBS and transferred into 15 ml falcon tubes. Two additional washing steps with wash I buffer (10 mM HEPES, 10 mM EDTA, 0.5 mM EGTA, 0.25 % Triton X-100) and wash II buffer (10 mM HEPES, 200 mM NaCl, 1 mM EDTA, 0.5 mM EGTA) were performed before resuspending the cells in 800 µl lysis buffer (50 mM Tris pH 8, 10 mM EDTA, 1 % SDS, 0.1 mM PMSF, and cOmplete EDTA-free protease inhibitor cocktail (Sigma Aldrich)). After 2 hours the cell lysates were sonicated using the bioruptor from Diagenode for 3×7 cycles (30 sec on– 30 sec off) at high frequency and centrifuged twice for 15 minutes at 10 °C at 16000 ×g. The DNA concentration was measured using the NanoDrop method (Peqlab). Hybridoma supernatant, containing secreted

IFR9 specific antibodies or an appropriate amount of STAT2 or Pol II specific antibodies (appendix) were incubated with 25 µg chromatin diluted in 900 µl dilution buffer (16.5 mM Tris pH 8, 165 mM NaCl, 1.2 mM EDTA, 1% Triton X-100, 0.1% SDS, 0.1 mM PMSF, and cOmplete EDTA-free protease inhibitor cocktail (Sigma Aldrich)) over night at 4 °C on a rotator. 50 µl magnetic beads per sample were blocked overnight in dilution buffer containing 1 % BSA. The next day, the beads were added to each sample and incubated for 2-3 hours at 4 °C washed with RIPA buffer (50 mM Tris HCL pH 8, 150 mM NaCl, 1% NP-40, 0.1% SDS, 0.5% sodium deoxycholate, 1 mM DTT), High Salt buffer (50 Mm Tris pH 8, 500 mM NaCl, 0.1% SDS, 1% NP-40), LiCl buffer (50 mM Tris pH 8, 250 mM LiCl, 0.5% sodium deoxycholate, 1% NP-40) and TE buffer (10 mM Tris pH 8, 1 mM EDTA) for 10 minutes at 4 °C. The proteins were eluted in freshly prepared elution buffer (2% SDS, 100 mM $NaHCO_3$, 10 mM DTT). The crosslink between proteins and DNA was reversed by adding 200 mM NaCl to each sample and incubation at 65 °C at 300 rpm for 12-16 hours. To digest the proteins, Proteinase K, 40 mM Tris pH 8 and 10 mM EDTA were added to each sample and incubated for 1 hour at 55 °C and 850 rpm. Each sample was transferred to phase lock tubes (5Prime), mixed 1:1 with phenol-chloroform-isoamylalcohol (PCI) and centrifuged for 5 minutes at 12000 ×g to extract nucleic acids. The water phase containing the nucleic acids was transferred to a new Eppendorf tube and mixed with 800 µl 96% Ethanol, 40 µl 3M CH_3COONa pH 5.3 and 1 µl Glycogen and stored for at least 2 hours or overnight at -20 °C. Next, each sample was centrifuged for 45 minutes at 4 °C and 16000 ×g. The pellet was washed in ice cold 70% ethanol and dried at 65 °C, before diluting the DNA in 100 µl H_2O. To better solubilize the DNA, each sample was shaken for 10 minutes at 65 °C and stored overnight at -20 °C.

qPCR for Analysis of ChIP samples

The ChIP samples were analysed by quantitative real-time PCR using the Eppendorf Realplex mastercycler and the SYBR KAPA mix (KAPA SYBR® FAST qPCR Kits, KapaBiosystems). The following PCR program was used: 95 °C for 2 min, 35× (95 °C for 15 sec, 60 °C for 15 sec, 72 °C for 15 sec), 95 °C for 15 sec, from 60 °C to 95 °C in 20 min for the melting curve, 60 °C for 2 min. Primers for the Mx2, IRF7, IRF1 3'UTR and IRF8 3'UTR genes were used. The data were normalized to the input.

SDS Polyacrylamide Gel Electrophoresis

5 µl size marker (Prestained PageRuler, Thermo Pierce #26619) and 20-50 µg samples were loaded onto gels. Gels were run at 80 V until the proteins ran through the 5% stacking gel (5% Acrylamide/Bisacrylamide, 0,125M Tris/HCl pH6,8, 0,2% sodium dodecylsulphate (SDS), 0,3% TEMED, 0,06% Ammonium persulfate (APS)), reached the 10% separating gel (7,5% acrylamide/bisacrylamide, 0,375M Tris/HCl pH8,8, 0,2% sodiumdodeyclsulphate (SDS), 0,3% tetramethylethylendiamin (TEMED), 0,06% Ammonium persulfate (APS)) and then were run at 120 V. The gels were run in 1x running buffer (25 mM Tris, 192 mM glycine, 0.1% SDS).

Semi-Dry Western Blot

The proteins were blotted on a nitrocellulose membrane (whatman ba-s-83 optitran) using the BioRad blotting aperture for 1.5 hours at 32 mA per gel. Separate stacks of whatman paper have been soaked in cathode buffer (40 mM 6-Aminocapronic Acid, 20% Methanol, 0.01 % SDS), anode buffer 1 (300 mM Tris, 20% Methanol, pH 10.4) or anode buffer 2 (2.5 mM Tris, 20% Methanol, pH 10.4) and assembled as shown below.

Cathode (-)
6× Whatman paper (with cathode buffer)
3× Whatman paper (with cathode buffer)
Separating gel (equilibrated in cathode buffer)
Nitrocellulose membrane (equilibrated in water)
6× Whatman paper (with anode buffer II)
3× Whatman paper (with anode buffer I)
Anode (+)

After blotting, the membranes were stained with Ponceau red (0.2% Ponceau S, 3% Trichloracetic acid) to check the quality of the protein transfer. The stained membranes were washed with water and TBS-T buffer (10 mM Tris-HCl pH 7.5, 150 mM NaCl, 0.05% Tween 20) and blocked in 5% milk powder dissolved in TBS-T buffer for 1 hour at room temperature. After blocking, the membrane was washed three times for 10 minutes in TBS-T and then incubated with the primary antibody over night at 4 °C. The next day the membrane was washed in TBS-T and then incubated with an

appropriate secondary antibody for 1 hour at room temperature. The membrane was washed again and proteins were detected using the Odyssey infrared imager (Licor) for fluorophore-coupled antibodies or detection on film for horseradish peroxidase (HRP)-coupled antibodies.

Tank Western Blot

After SDS-PAGE, the proteins were blotted on a PVDF (Millipore) membrane at 4 °C for 16 hours at 200 mA and for 2 hours at 400 mA using a peqlab apparatus. The PVDF membrane was first activated for 10 seconds in 96% EtOH and then equilibrated in carbonate transfer buffer (3 mM Na2CO3, 10 mM NaHCO3, 20% ethanol) for 30 minutes. The gel was also equilibrated in carbonate buffer. Sponges and Whatman paper were soaked in transfer buffer. The transfer cassette was assembled as indicated:

Cathode (+)
1x sponge
3x Whatman paper
SDS gel
Activated membrane
3x Whatman paper
1x sponge
Anode (-)

To check the efficiency of the transfer, the member was stained with Ponceau S and washed with water and TBS-T. To fix the proteins, the membrane was plunged into 96% Ethanol and dried for 30 minutes. The membrane was reactivated by immersing it into Ethanol for 10 seconds and blocked in 5% milk powder in TBS-T for 1 hour at room temperature. The membrane was washed three times with TBS-T and then incubated with the primary antibody over night at 4°C while shaking. The next day the membrane was washed again and incubated with an appropriate secondary antibody for 1h at room temperature. The membrane was analysed with the Odyssey infrared imager (Licor) for fluorophore-coupled antibodies or detection on film for horseradish peroxidase (HRP)-coupled antibodies.

Luciferase Assay

1.5 x10^5 mouse embryonic fibroblasts (MEF) per well were seeded in a 6-well plate and transfected with 2-5 µg plasmids DNA, containing myc-tagged p65 and IRF9,

using Turbofect (Thermo Scientific). Either a firefly luciferase-based NFκB or ISGF3 reporter construct was co-transfected.

Luciferase activity of the NFκB [102] and ISGF3 reporter was measured with the Dual Luciferase Reporter Assay System (Promega).

Cells were lysed with 1× passive buffer. LAR II solution, containing beetle luciferin, a substrate for the firefly luciferase, was added to 20 µl of each sample and the luciferase activity was measured with a luminometer. Next, 100 µl “Stop & Glow” stop solution, containing coelenterazine, the substrate for the *Renilla* luciferase, was added to the mix and luciferase activity was measured again.

The data was normalized to the *Renilla* luciferase activity and an empty vector control sample.

Results

Analysis of TNF as a second stimulus for genes co-ordinately regulated by NFκB and ISGF3.

In order to separate the NFκB and JAK/STAT signaling pathways while studying NFκB and ISGF3 coregulated genes, such as *Nos2*, cells are treated with hkL and IFN-β. Cells treated with hkL alone or together with IFN-β show the expected expression pattern of *Nos2*, specifically, a highly increased *Nos2* expression after double treatment compared to hkL alone [96]. However, it is unclear whether the recognition of hkL by PRR exclusively activates the NFκB signaling pathway or if other pathways are also involved in changing the cells expression profile.

To test this, the expression of NFκB and ISGF3 target-genes was quantified using quantitative PCR in RAW 264.7 cells, a murine-leukemic monocyte-macrophage cell line. Cells were treated with hkL, IFN-β and TNF-α. TNF is produced as a result of hkL treatment and activates the pathway. To test the synergism with IFN-b, hkL/IFN-β and TNF-α/IFN-β double-treatments were performed for 4h.

Figure 8 shows the expression levels of the coregulated genes iNOS and IL-6, the NFκB-dependent gene IκB-α, and the interferon stimulated genes Mx1 or Mx2. Indeed, hkL is able to induce the expression of NFκB-dependent genes, but not ISGs. Furthermore, the expression of coregulated genes is highly increased after hkL/IFN-β co-treatment, compared to hkL alone. However, TNF-α fails to induce any gene expression, even in higher concentrations and longer treatments (data not shown). Even though RAW 264.7 cell line should be comparable to bone marrow or splenic macrophages, regarding cell surface receptors [103] and ability to produce TNF-α after LPS stimulation [104], a possible explanation for its unresponsiveness to TNF-α treatment could be due to the lack of TNF-α receptor (TNFAR) expression. To pursue this question, the same experimental setup has been repeated with bone marrow-derived macrophages (Figure 9). These macrophages show the same expression patterns for the tested genes as the RAW 264.7 cells after hkL and hkL/IFN-β treatments, but with a much higher induction rate. Furthermore, TNF-α induces the expression of NFκB-dependent genes in BMDM. However, the effect is much weaker than hkL.

First, these results indicate that RAW 264.7 cells are either unable to express the TNFAR or unable to respond to its stimulation. Additionally, even though hkL have a stronger effect on NFκB-dependent genes and coregulated genes than TNF-α, the expression of coregulated genes is highly increased after the co-treatment with TNF-α and IFN-β compared to TNF-α alone. Possibly, the recognition of hkL by PRR also stimulates other pathways that synergize with IFN-b. Recognition of *L. monocytogenes* by PRR was shown to also activate the MAPK pathway [105, 106]. During a study in our lab, MAPK pathways downstream of PRR targeting ERK, JNK and p38MAPK were inhibited with pharmacological drugs during *L. monocytogenes* infection. However, this didn't show any reduction of *L. monocytogenes* induced *Nos2* expression [96]. Furthermore the activation and kinetics of NFκB upon an infection and cytokine treatment might differ, thus explaining the disparities in induction levels.

Although the induction rates of hkL and TNF-α on coregulated gens differ, the results show that separating the NFκB and JAK/STAT signaling pathways by replacing hkL with TNF as a costimulus with IFN-b is a suitable tool for the study of NFκB and ISGF3 coregulated genes.

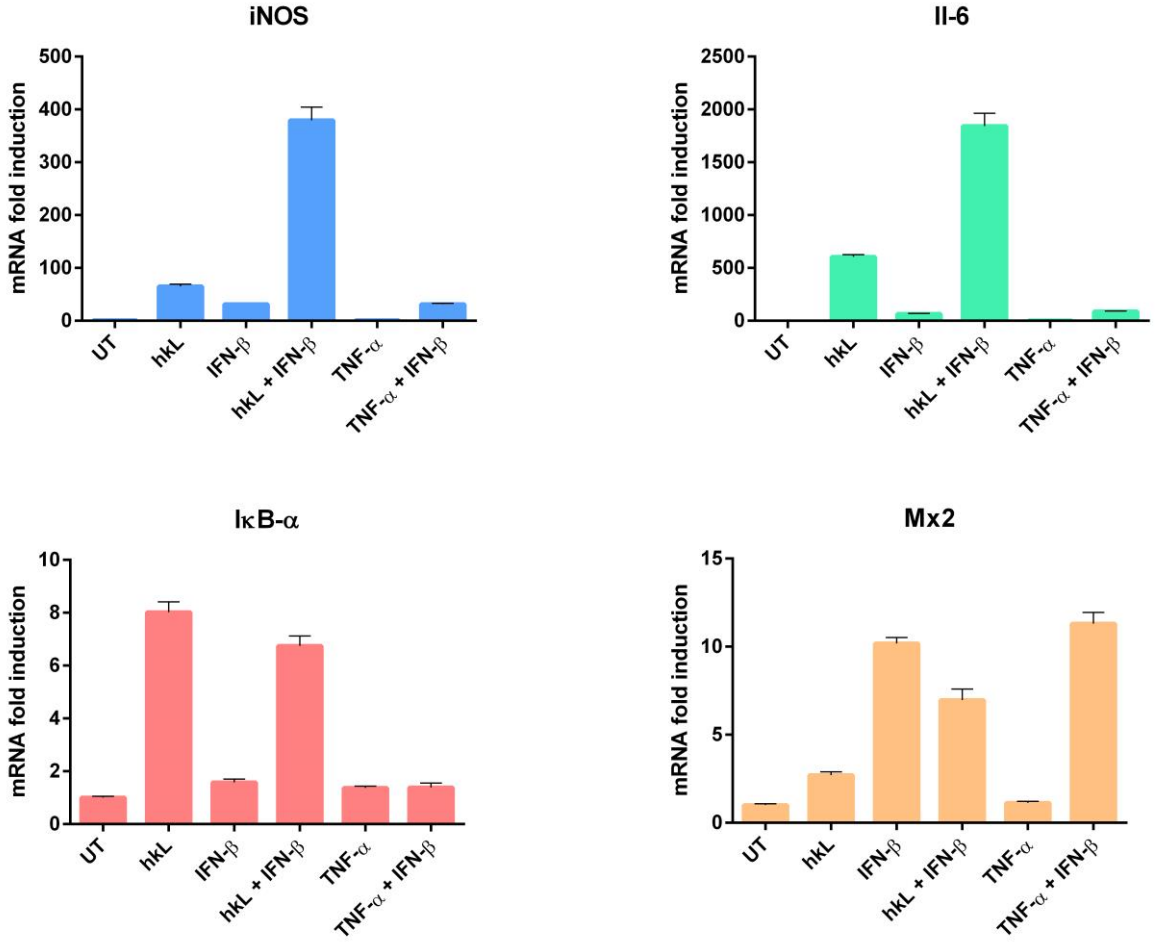

Figure 8: **Quantitative analysis of iNOS, IL-6, IκB-α and Mx2 mRNA expression levels in RAW 264.7 cells.** RAW 264.7 cells were treated with hkL, TNF- α, IFN-β or hkL/IFN-β and TNF-α/IFN-β double-treatments for 4h. mRNA was isolated, reversely transcribed into cDNA and analysed by qPCR.

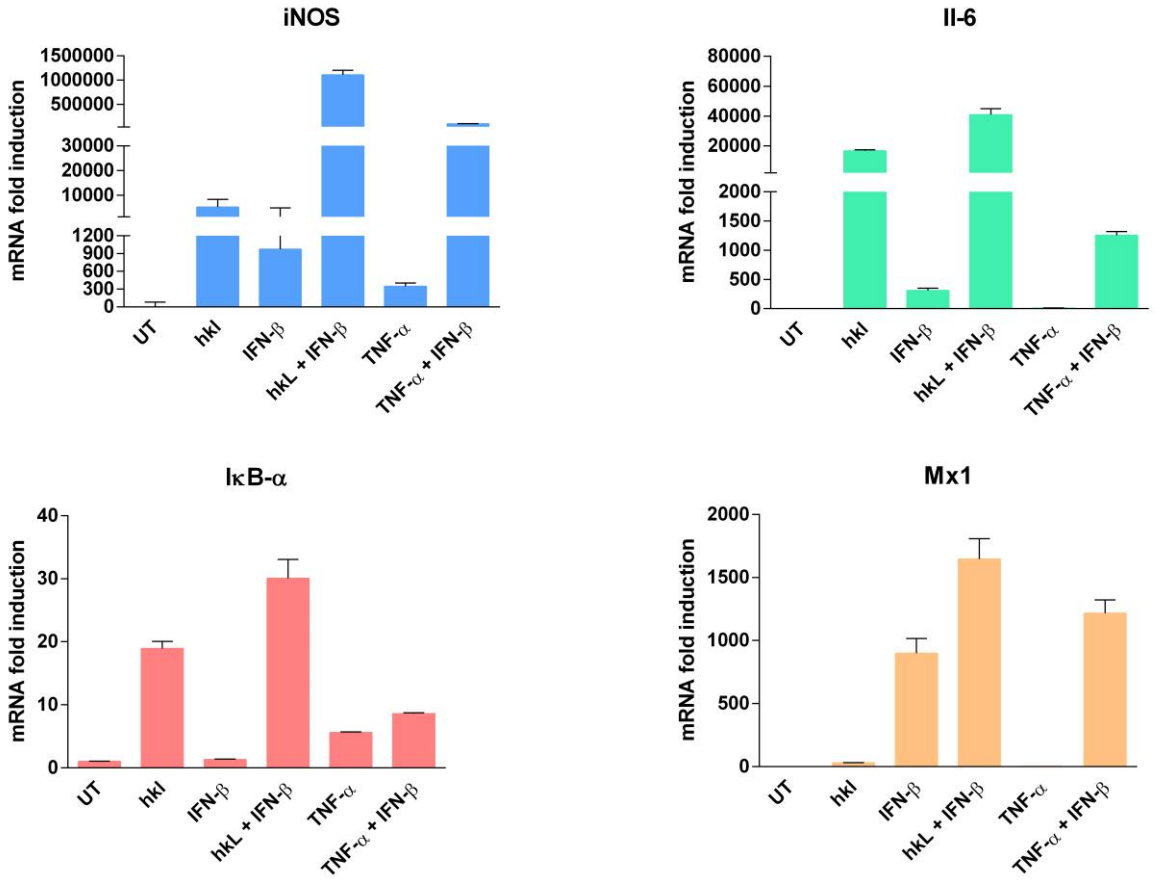

Figure 9: **Quantitative analysis of iNOS, IL-6, IκB-α and Mx2 mRNA expression levels in BMDMs.** Bone marrow-derived macrophages (BMDMs) were treated with hkL, TNF- α, IFN-β or hkL/IFN-β and TNF-α/IFN-β double-treatments for 4h. mRNA was isolated, reversely transcribed into cDNA and analysed by qPCR.

Investigation of an NFκB p65 and CDK7 interaction

Expression of CDK7-GST and NFκB p65-GST Fusion Proteins and examination of their interaction.

One of our recent studies has shown an NFκB-dependent recruitment of TFIIH/CDK7 and colocalization of these factors on the *Nos2* promoter after treatment with hkL alone and hkL/IFN-β double-treatment [96]. To test whether this NFκB-dependent recruitment of CDK7 to the promotor is a result of a direct interaction between the p65 and CDK7, a GST pull-down assay was designed, where GST-tagged p65 and CDK7 would be used to capture the respective interaction. For this purpose, constructs encoding the GST-tagged proteins were generated and introduced into an E. coli strain under an IPTG-inducible promoter.

Even after the expression of the constructs in different solubility enhancing E. coli strains (Rosetta pLysS, SoluBL21), the expressed proteins were highly insoluble. Therefore, different IPTG concentrations (0.1-1.0 mM), ampicillin concentrations (50 µM, 100µM), media (LB, 2XYT) and temperatures (18°C, 37°C) were tested without obtaining a reasonable amount of soluble GST-tagged proteins (Figure 10; not all conditions shown). Even though the GST-tag is known to enhance the solubility of fusion proteins [107], this characteristic is not displayed in combination with p65 and CDK7. Whereas a band for GST-tagged CDK7 can be seen at the predicted height (67 kDa) after Coomassie staining, the band for the full length GST-tagged p65 (87kDa) could only be detected by western blot with a p65-specific antibody (data not shown). After Coomassie staining only a truncated version of p65 could be detected (~70kDa). This is an indication that beside the solubility issue, GST-tagged p65 also gets rapidly degraded, turning it useless for the purpose of a GST pull-down.

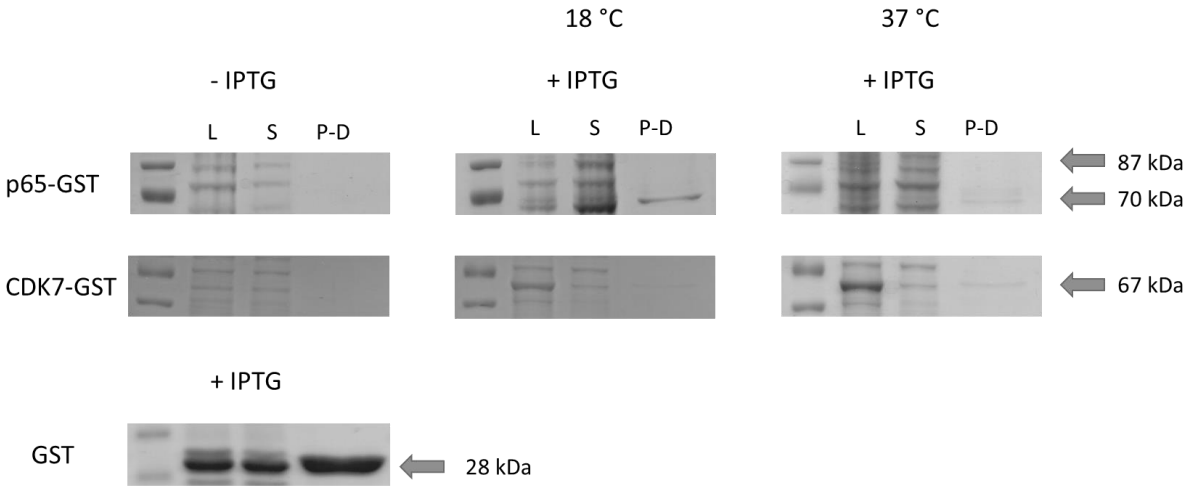

Figure 10: Expression of GST-tagged proteins. Coomassie staining of GST-tagged p65 and CDK7, expressed in IPTG-inducible Rosetta pLysS E. coli strain, at 18°C or 37°C. Full length GST-CDK7, but not GST-p65 can be detected. L: complete Lysate; S: supernatant containing the soluble protein fraction; P-D: GST-tagged proteins, pulled-down with glutathione magnetic beads.

After trying a variety of different conditions without achieving a higher solubility, we decided to shift from a GST pull-down assay to a co-immunoprecipitation of overexpressed myc- and HA-tagged proteins in HEK293 cells. Alternatively, it would have been possible to switch from a bacterial expression system to an insect or eukaryotic system or use a different tag, such as a MBP-tag [108], which could further enhance

the solubility of the fusion protein. This would probably resolve the solubility and degradation issues, but would also be more cost-intensive and time-consuming.

Co-immunoprecipitation of the NFκB subunit p65 and CDK7

For the switch to the co-immunoprecipitation approach of overexpressed proteins, several constructs containing myc- and HA-tagged proteins needed to be generated (shown in Table 1). In addition, an immunoprecipitation protocol had to be established to ensure a genuine interaction between overexpressed proteins. Available protocols using Frackelton buffer as a lysis buffer could not be used, since the stringency of the buffer was not strong enough to break the nuclear membrane of the cells. The nuclear fraction was of big interest, since some of the overexpressed proteins, including p65 and IRF9, contain a nuclear localization signal, enabling them to shuttle to the nucleus. Indeed, overexpressed p65 (second, upper p65 band) could not be detected via western blot when the cells were lysed with a non-denaturing lysis buffer, such as the Frackelton buffer, but could be detected after lysis with stringent Laemmli buffer (Figure 11). In contrast, endogenous p65 (single, lower p65 band) was detected via western blot after cell lysis with any buffer (Figure 11). Most probably overexpressed p65 was not bound by its inhibitor κB (IκB) to prevent it from shuttling to the nucleus, because the number of p65 greatly exceeds the number of available IκB. A balance between the buffer being stringent enough to breach the nuclear membrane, but not too harsh to disrupt the protein interactions had to be found. After having tested a variety of non-denaturing and denaturing buffers, a RIPA buffer without SDS was shown to disrupt the integrity of the nuclear membrane but not the protein interaction and was chosen for the immunoprecipitation of overexpressed proteins.

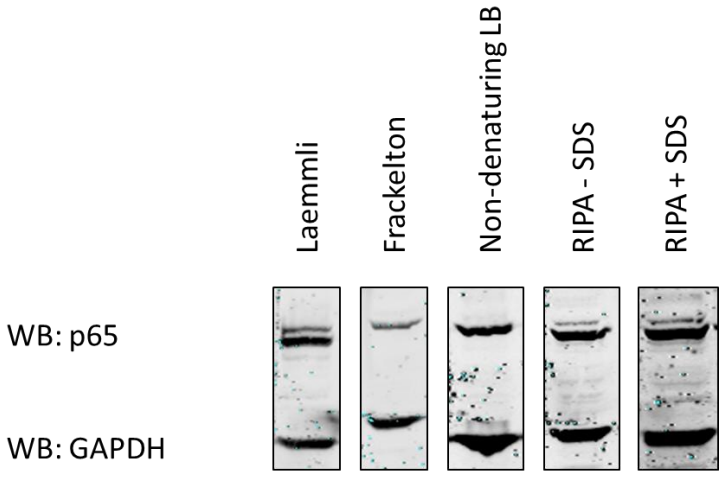

Figure 11: Detection of overexpressed HA-p65 after cell lysis with different buffers. Overexpressed p65 (second, upper band) is only detected after HEK293 cells were lysed with Laemmli or RIPA buffer, not with the non-denaturing buffers. The lower or single band represents the endogenous p65.

Proteins were overexpressed in HEK293 cells and immunoprecipitated using myc-, HA- and p65-specific antibodies. The precipitated proteins were analysed by western blot (Figure 12).

Myc-CDK7 and HA-p65 were co-immunoprecipitated using a myc, HA or p65 antibody, respectively. However, it appeared that the immunoprecipitation with the HA antibody was not as efficient as with the myc- and p65 antibodies. This is probably due to the lesser quality of the HA antibody, since the more sensitive SuperSignal™ West Femto Maximum Sensitivity Substrate (ThermoFischer Scientific) was needed for the detection of the HA-tagged proteins. In contrast, p65 and myc-tagged proteins were detected using the less sensitive SuperSignal™ West Pico Chemiluminescent Substrate (ThermoFischer Scientific). As positive controls, CDK7 was also co-immunoprecipitated with cyclin H (cycH) and p65 with p50. In the p65 immunoprecipitation it appears that a small amount of p65 produces a strong signal for p50. This is most probably also due to different qualities of antibodies, since a more sensitive kit was needed for the detection of HA-tagged proteins compared to myc-tagged proteins. CDK7 and cyclin H form a trimeric complex with MAT1, which functions as a CDK-activating kinase (CAK) and is an essential component of the transcription factor TFIIH. IRF9 was considered to serve as a negative control for both CDK7 and p65. Although CDK7 could indeed not be co-immunoprecipitated with IRF9, p65 and IRF9 were surprisingly both detected by western blot when targeting p65 for precipi-

tation. Screening the literature more carefully revealed that this interaction has previously been shown *in vitro* [57]. In summary, both CDK7 and IRF9 were found to interact with p65. However, these results can still only count as an indication, since additional negative controls are needed to fully confirm the genuineness of these interactions. Additionally, these results have not yet been reproduced due to time constraints. Furthermore, the blots are compromised with spill-overs from neighbouring lanes. However, these bands can easily be distinguished from the legitimate ones. In spite of the limitations of the experiment, the results indicate an interaction between p65 and CDK7 as well as between p65 and IRF9. The implication of the later interaction is not known. Drew P.D et al. (1995) showed that NFκB physically interacts with IRF2 to inhibit NFκB induction of major histocompatibility complex I and β2-microglobulin gene expression [57]. The question whether IRF9 could also inhibit NFκB target gene expression arose and was investigated with an NFκB reporter gene assay.

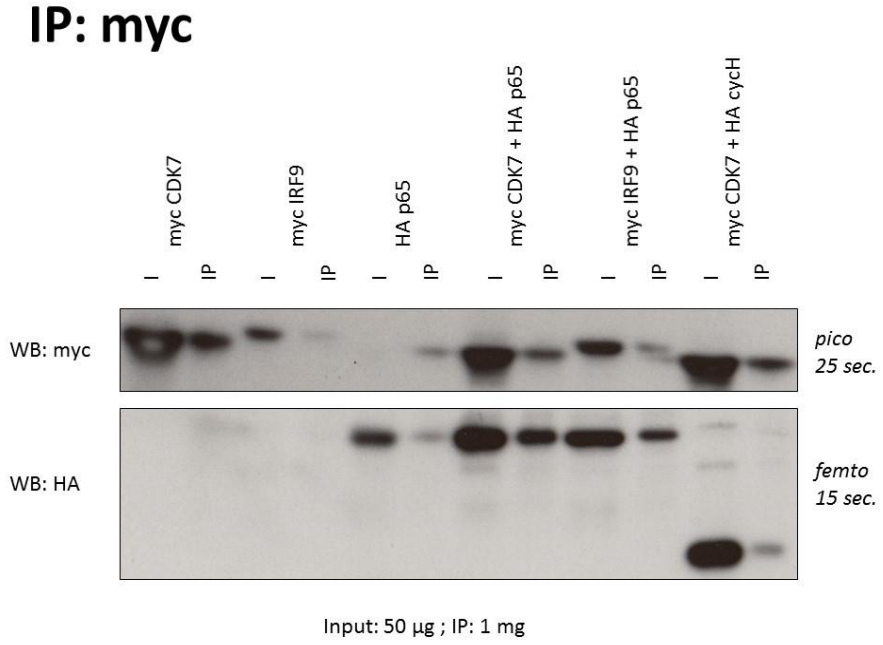

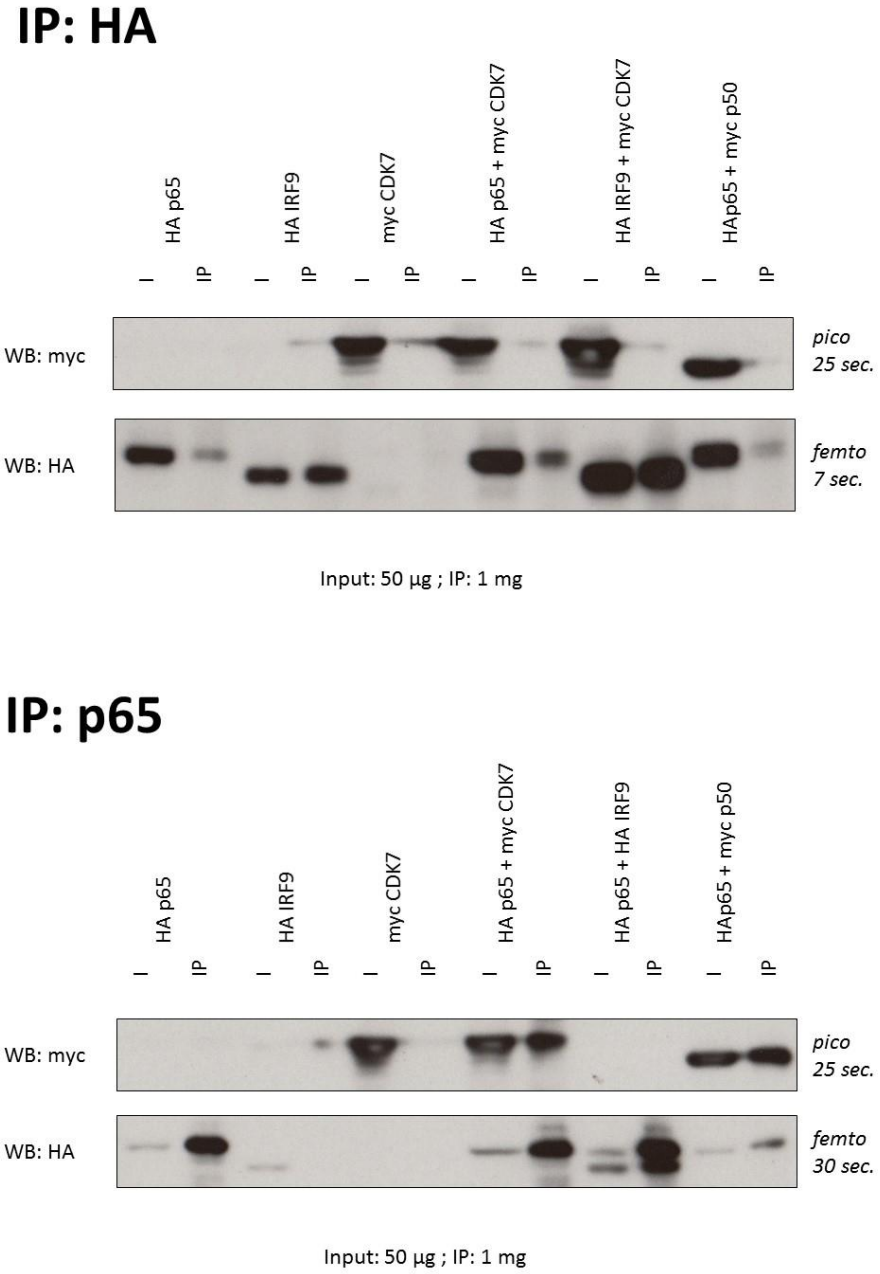

Figure 12: Co-immunoprecipitation of p65 and CDK7. HEK293 cells were transiently transfected with myc- and HA-tagged proteins. The overexpressed proteins were precipitated using myc-, HA- or p65-specific antibodies and detected by western blot with myc- and HA-specific antibodies. As input (I) 50 µg of complete lysate was loaded. 1 mg of protein was used for immunoprecipitation (IP).

IRF9 has no impact on NFκB activation

To pursue the question whether IRF9 interacts with NFκB to inhibit NFκB target gene induction, p65 and IRF9 were transiently co-transfected in Wt MEFs with an NFκB or ISRE reporter (Figure 13). The firefly luciferase activity was measured and normalized to the Renilla luciferase activity and to the empty vector control. The ISRE re-

porter gene assay functions as a negative control, since neither p65, nor IRF9 alone without Stat1 or Stat2 should induce the ISRE reporter gene. As expected, p65 induces the NFκB reporter gene activity. However, IRF9 has no impact on NFκB activation, when p65 and IRF9 are co-transfected.

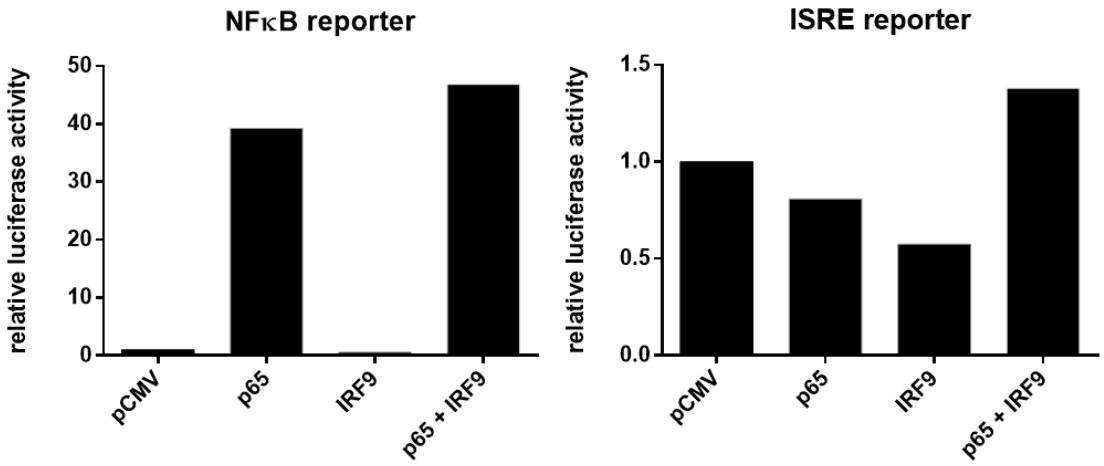

Figure 13: Influence of IRF9 on NFκB activation. HEK 293 cells were co-transfected with p65, IRF9 and an NFκB or ISRE reporter. Firefly luciferase activity was measured and normalized to the Renilla luciferase activity. The graphs do not show any SD or SE, since this experiment has only been performed once.

Generation of a monoclonal IRF9 Antibody

Overexpression of IRF9 in *E. coli*

In the past years, some non-canonical pathways involving IRF9 have been identified [50-52]. For the investigation of the role of ISGF3 in the induction of NFkB synergy genes and for examining IRF9-dependent genes and characterization of IRF9-dependent canonical and non-canonical IFN pathways, a ChIP-grade monoclonal IRF9 antibody would be a valuable tool. Since we were not able to obtain good results with any commercially available antibody, we started to generate a monoclonal murine IRF9 antibody in cooperation with the Ogris lab. The first step in the generation of the IRF9 antibody was to clone murine IRF9 into a pET-Duet or pET23a+ plasmid containing an N- or C-terminal His-tag, respectively. His-tagged IRF9 was then expressed in the *E. coli* Rosetta pLysS strain and purified using Ni-sepharose beads. The concentration and purity of the His-tagged IRF9 was evaluated with a BSA concentration gradient (Figure 14) and a BCA assay.

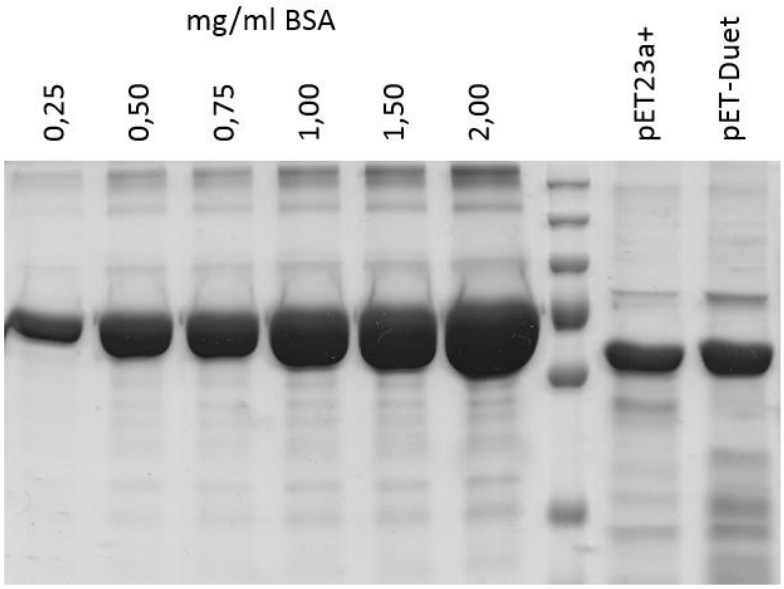

Figure 14: Expression of His-tagged IRF9. C- and N-terminal His-tagged IRF9 was expressed in *E. coli* and purified using Ni-sepharose beads. The concentration and purity of His-IRF9 was compared to a BSA concentration gradient and estimated to be between 0.25 - 0.50 mg/ml. pET23a+ contains the C-terminal and pET-Duet the N-terminal His-tag.

Test of polyclonal IRF9 antibodies from mouse sera

To anticipate the case that either the N- or C-terminal tagged IRF9 would initiate a much stronger immune response, two mice were immunized with each variant. After several rounds of immunization, the serum from the second bleeding of mice was tested via western blot on Wt MEF lysates transfected with myc-IRF9 (Figure 15) and via ChIP on BMDMs treated with IFN-γ overnight and IFN-β for 2 hours (Figure 16).

On western blot (done by the Ogris lab), the serum gained from the 2nd bleedings was compared to the serum from the 1st bleedings. Furthermore, the pre-immunization serum was included as a negative control. To prove that the transfection has been successful and that myc-IRF9 is indeed expressed, the blot was incubated with a monoclonal myc tag-specific antibody (Ogris lab). To further examine the quality of our homemade antibody, a polyclonal antibody provided by David Levy was included as a positive control. The strongest signal was achieved by using the serum of mouse #2 (M2), whereas M1 showed the weakest signal. However, the strength of the signal does not necessarily reflect the affinity of the antibody, but could also be caused by variations in the antibody concentration of the sera. Myc-IRF9 is detected above the 50 kDa maker band, proving that the transfection has

been successful. However, a second strong band below the myc-IRF9 band was observed. This is most probably a product of IRF9 degradation.

To test whether the polyclonal antibody is suitable for chromatin immunoprecipitation experiments, BMDMs were primed with IFN-γ overnight to induce the expression of IRF9 [109, 110]. The next morning the cells were treated with IFN-β for 4 hours. Upon IFN-β treatment, STAT1 and STAT2 are phosphorylated by JAKs and form the ISGF3 complex with IRF9, which translocates to the nucleus and binds to Interferon-stimulated response elements in the promoter region of ISGs (e.g. MX2, IRF7). The sera from four different mice, which have been immunized with IRF9 (M1-M4), were tested for their quality to bind chromatin-bound IRF9 (Figure 16 and 17). The pre-immunization serum from different mice functioned as a negative control, since they should not contain any IRF9-specific antibodies. Additionally, an irrelevant site on the DNA for the binding of IRF9 (IRF8 3'UTR) was tested as a negative control. Since IRF9 binds the DNA together with STAT1 and STAT2 as the ISGF3 complex, STAT2 functions as a positive control. In both tests the serum of M2 generated the highest and most consistent signal on the Mx2 and IRF7 ISRE. In contrast to this, M1 generated a strong signal for the IRF7 ISRE in the first test, but not the second (Figure 16). Similarly, M4 generated a strong signal on the Mx2 and IRF7 ISRE in the second test. Additionally, the M4 serum also generated a signal on the IRF8 3'UTR, which makes the signal obtained for Mx2 and IRF7 ISRE unreliable (Figure 17). Taken together, the results from the first and second test show that the M2 serum seems to be the best candidate for the generation of a monoclonal antibody. For this, hybridomas from antibody-producing B cells and myeloma cells for the production of monoclonal iRF9 antibodies had to be generated.

To make sure the signal is specific to IRF9, the sera were tested by western blot on Wt and IRF-/- MEFs (Figure 18). The strongest signal for the endogenous IRF9 (48 kDa) was observed with the M2 serum. M1 serum showed as well a strong signal, whereas almost no band could be observed with M3 and M4. Furthermore, no IRF9 band was detected in the IRF9 -/- MEF lysates.

Additionally, the M2 serum was tested again by ChIP in Wt BMDM treated with IFN-β for two hours and comparted to IRF9 -/- BMDMs (Figure 19). Indeed, M2 polyclonal IRF9 antibodies provide a strong signal on Mx2 and IRF7 ISREs in Wt BMDMs compared to IRF9 -/- BMDMs.

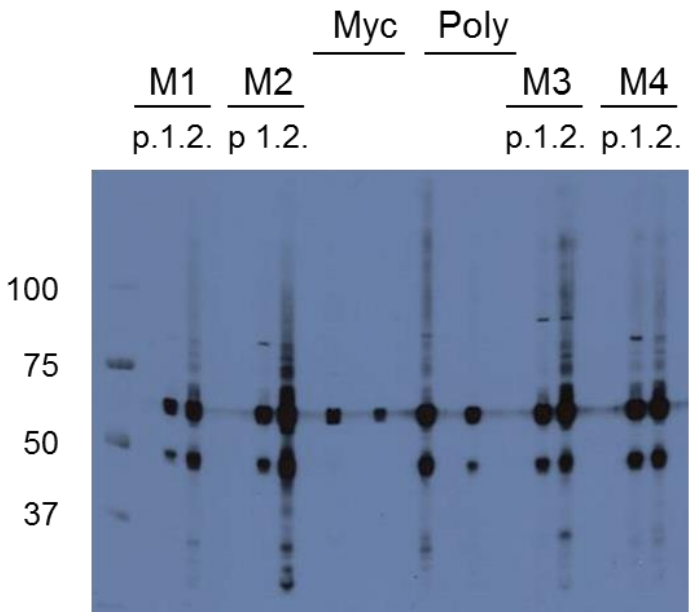

Figure 15: Test of polyclonal IRF9 antibodies. IRF9 polyclonal antibodies from the serum of immunized mice (M1-M4) were tested on lysates from IRF9 -/- MEFs, transfected with myc-IRF9. All mouse sera were diluted 1:500. The blots were exposed for 60 seconds. p: pre-immunization serum; 1: 1st bleeding; 2: 2nd bleeding; Myc: monoclonal myc AB (Ogris lab); Poly: polyclonal IRF9 AB (David Levy).

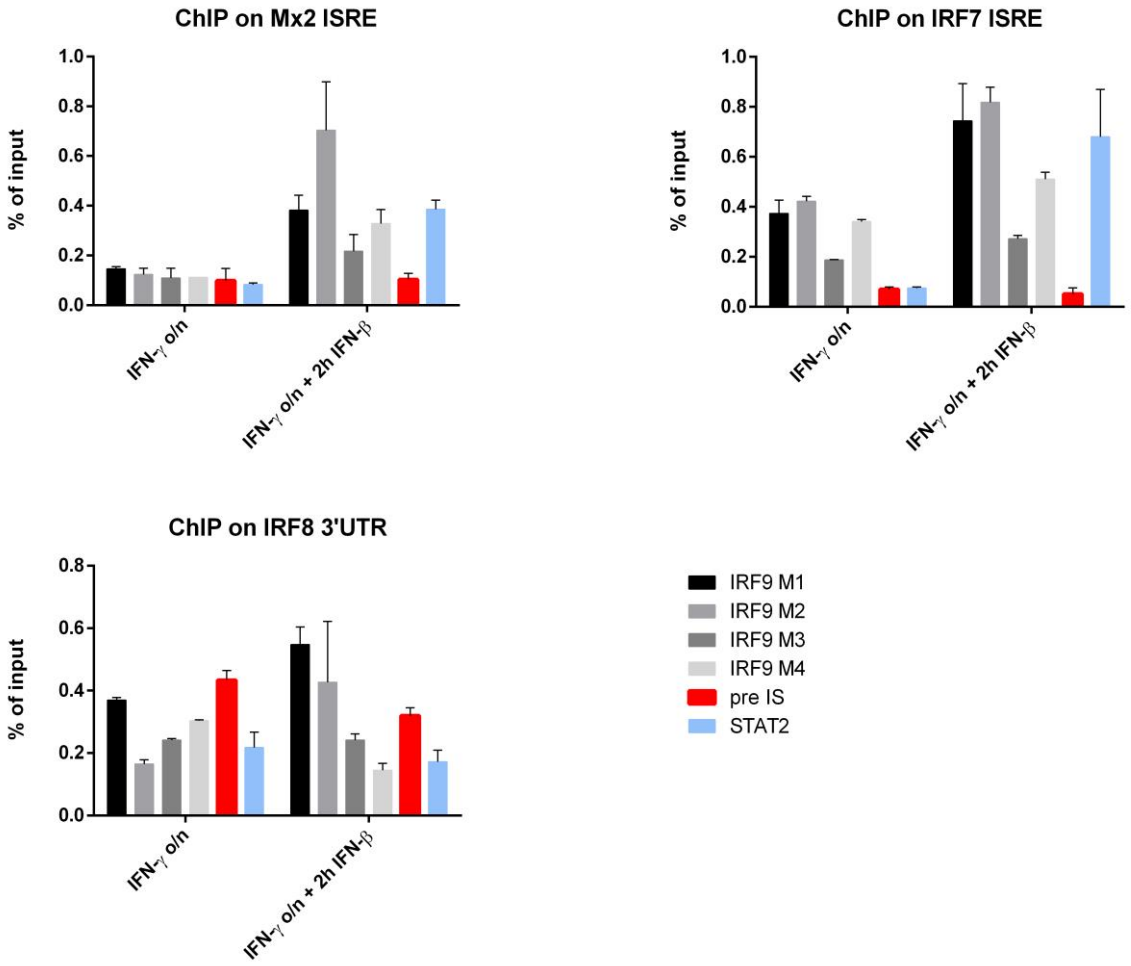

Figure 16: 1st ChIP to test polyclonal antibodies on the recruitment of IRF9 to the DNA of Wt BMDM after treatment with IFN-γ over-night and IFN-β for 2h. IRF9 was precipitated from the Mx2 and IRF7 gene ISRE using polyclonal antibodies originating from serum of the second bleed of four different mice (M1-M4), which have been immunized with overexpressed IRF9. STAT2 works as a positive control for the ISRE sites, whereas the pre-immune serum (pre IS) functions as a negative control. An additional negative control is the recruitment of IRF9 to the 3'UTR of the IRF8 gene. The serum of M2 worked best for the precipitation of IRF9 on the Mx2 and IRF7 ISRE, whereas M1 serum only showed to be promising on the IRF7 ISRE.

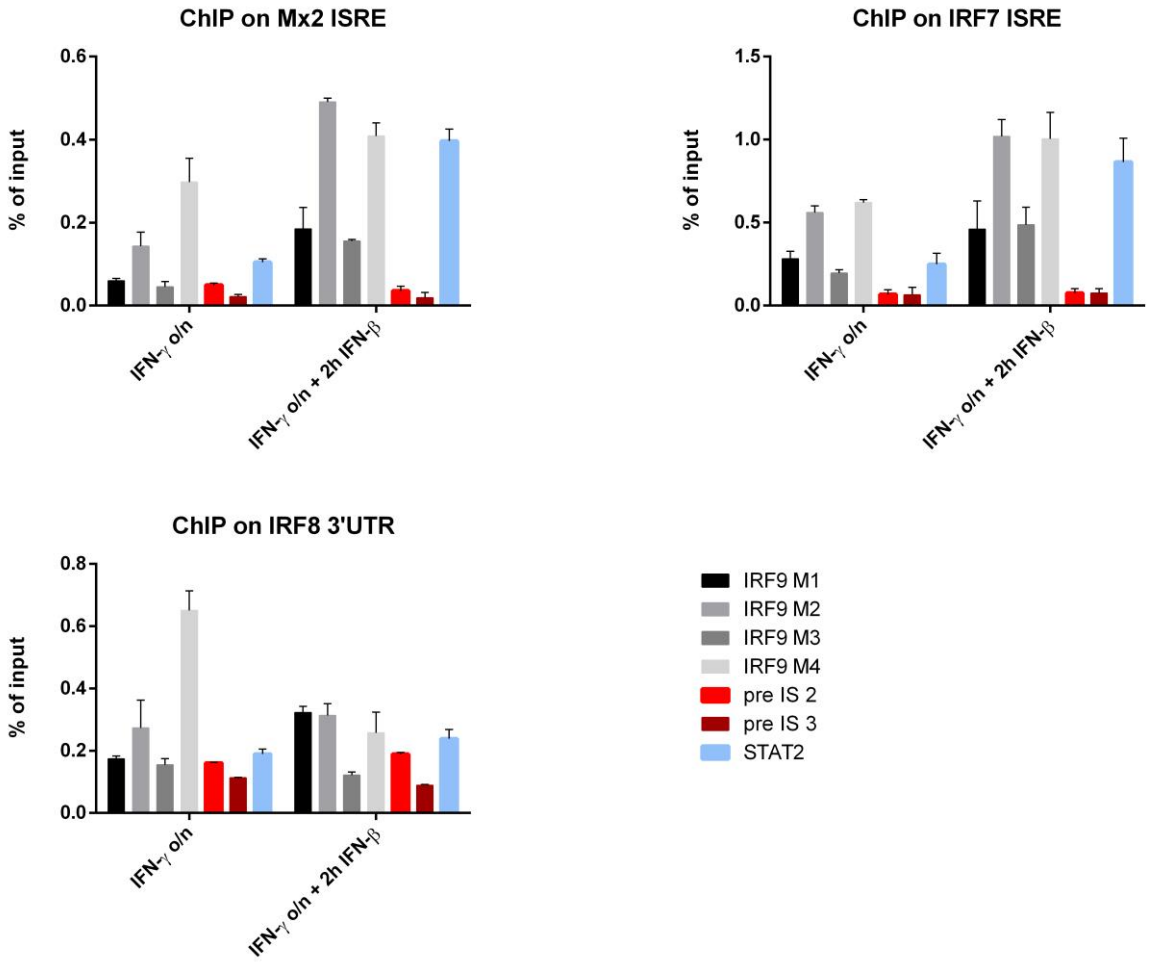

Figure 17: 2nd ChIP to test polyclonal antibodies on the recruitment of IRF9 to the DNA of Wt BMDM after treatment with IFN-γ over-night and IFN-β for 2h. IRF9 was precipitated from the Mx2 and IRF7 gene ISRE using polyclonal antibodies originating from serum of the second bleed of four different mice (M1-M4), which have been immunized with overexpressed IRF9. STAT2 works as a positive control for the ISRE sites, whereas the pre-immune serum (pre IS) functions as a negative control. An additional negative control is the recruitment of IRF9 to the 3'UTR of the IRF8 gene. The serum of M2 and M4 worked best for the precipitation of IRF9 on the Mx2 and IRF7 ISRE.

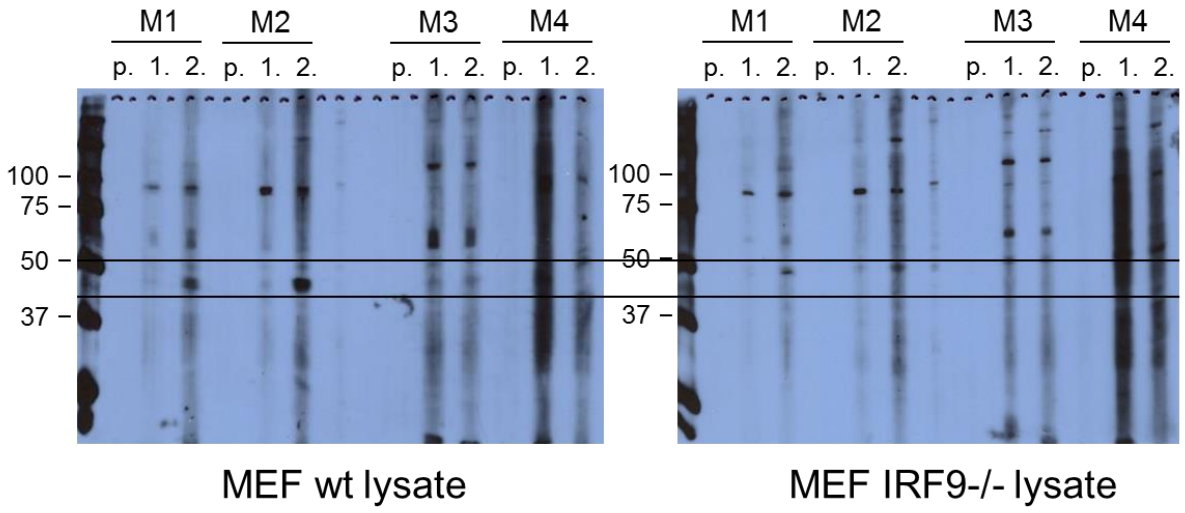

Figure 18: Test of polyclonal IRF9 antibodies on endogenous IRF9. IRF9 polyclonal antibodies from the serum of immunized mice (M1-M4) were tested on lysates from Wt vs IRF9 -/- MEFs. All mouse sera were diluted 1:500. The blots were exposed for 20 minutes. p: pre-immunization serum; 1: 1st bleeding; 2: 2nd bleeding; Myc: monoclonal myc AB (Ogris); Poly: polyclonal IRF9 AB (David Levy).

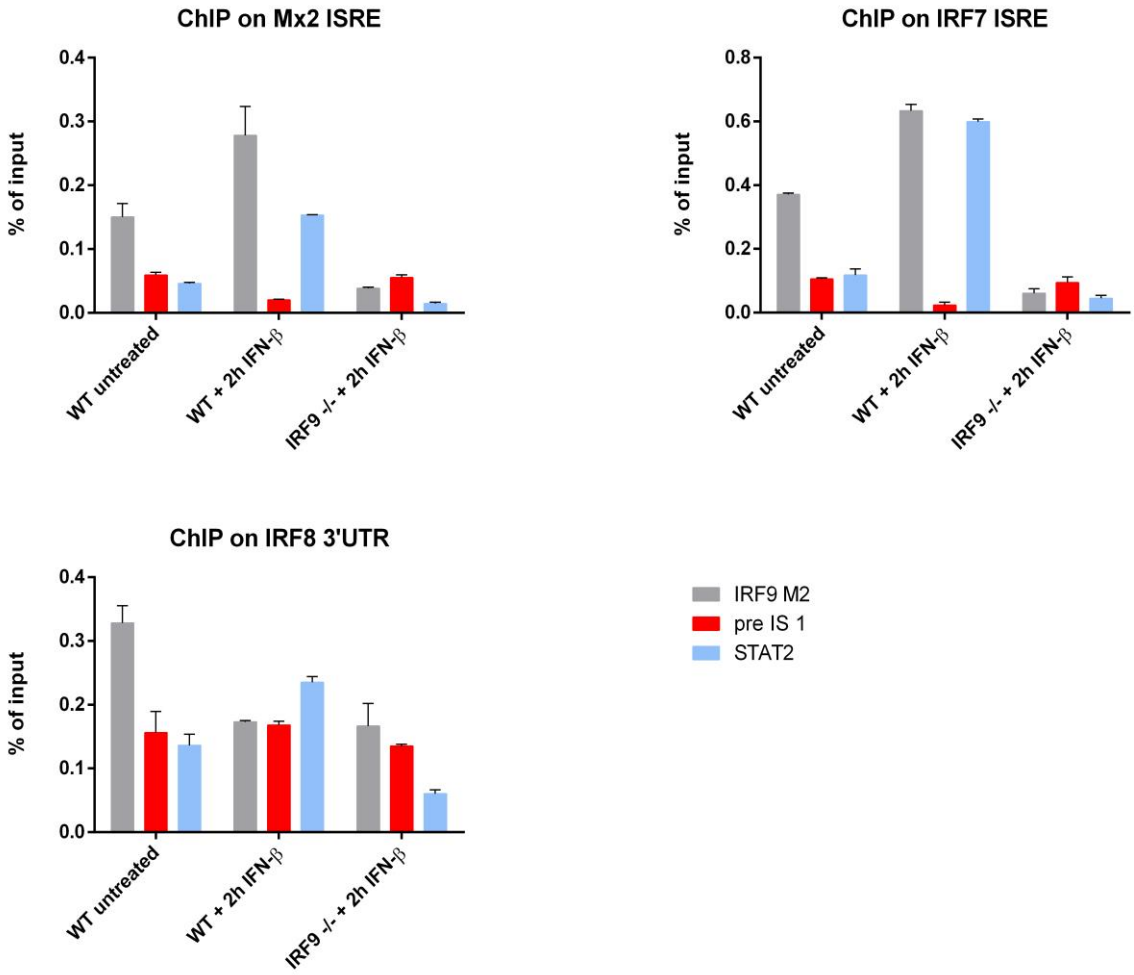

Figure 19: 3rd ChIP to test polyclonal antibodies on the recruitment of IRF9 to the DNA of Wt and IRF9-/- BMDM after treatment with IFN-b for 2h. IRF9 was precipitated from the Mx2 and IRF7 gene ISRE using polyclonal antibodies originating from serum of the second bleed of mouse 2 (M2), STAT2 works as a positive control for the ISRE sites, whereas the pre-immune serum (pre IS) functions as a negative control. An additional negative control is the recruitment of IRF9 to the 3'UTR of the IRF8 gene.

Test of hybridoma supernatants for reactivity with IRF9

After the first set of tests, M2 was chosen to be the best candidate for the isolation and fusion of antibody-producing B cells with myeloma cells, to render them immortal. A series of populations of polyclonal hybridoma cells was subsequently tested by western blot and immunoprecipitation (IP) for their specificity for IRF9. The western blot revealed fifteen promising polyclones which have been marked by a code (Figure 20). These candidates have been tested by IP on Wt MEFs transiently transfected with myc-IRF9 (Figure 21). All the candidates, except for 8E2 were able to precipitate IRF9. Especially the signal from the candidates 6F1 and 6H7 can be appreciated. Nevertheless, the antibody concentration may also vary for the different polyclones. Additionally, these candidates have been tested by ChIP, which was done by Ekaterini Platanitis (Figure 22). Here as well candidate 6F1 provided the highest signal and was used for the single cell titration.

The monoclonal antibodies from the single-cell clones were subsequently tested by western blot (Ogris) and ChIP (Ekaterini Platanitis) and the best working monoclonal antibody was kept as a final product (data not shown).

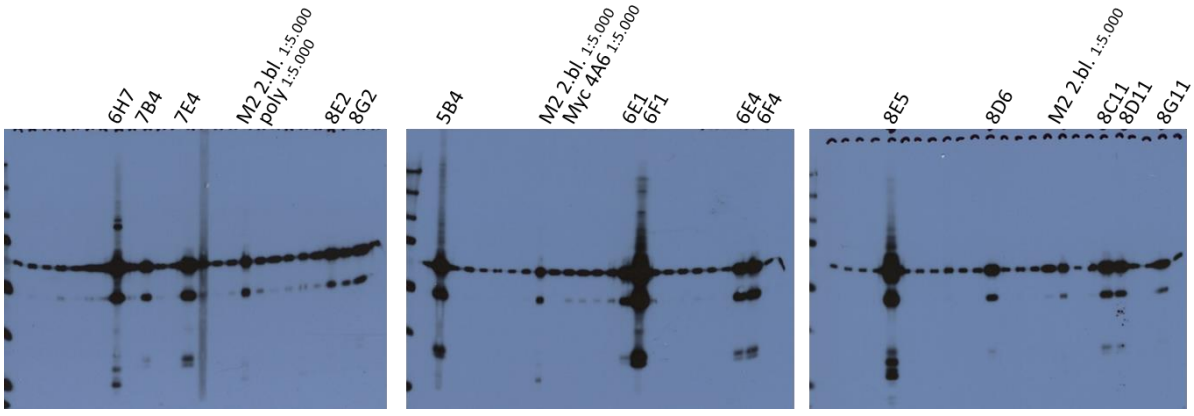

Figure 20: Western blot test of mixclone polyclonal antibodies on myc-IRF9. Antibody-producing B cells isolated from M2 were fused with myeloma cells to form hybridomas and divided into small mixclone populations. Undiluted culture supernatant containing the antibodies was used for the western blot. The blots were exposed for 3 minutes. Promising polyclones were subsequently tested by IP.

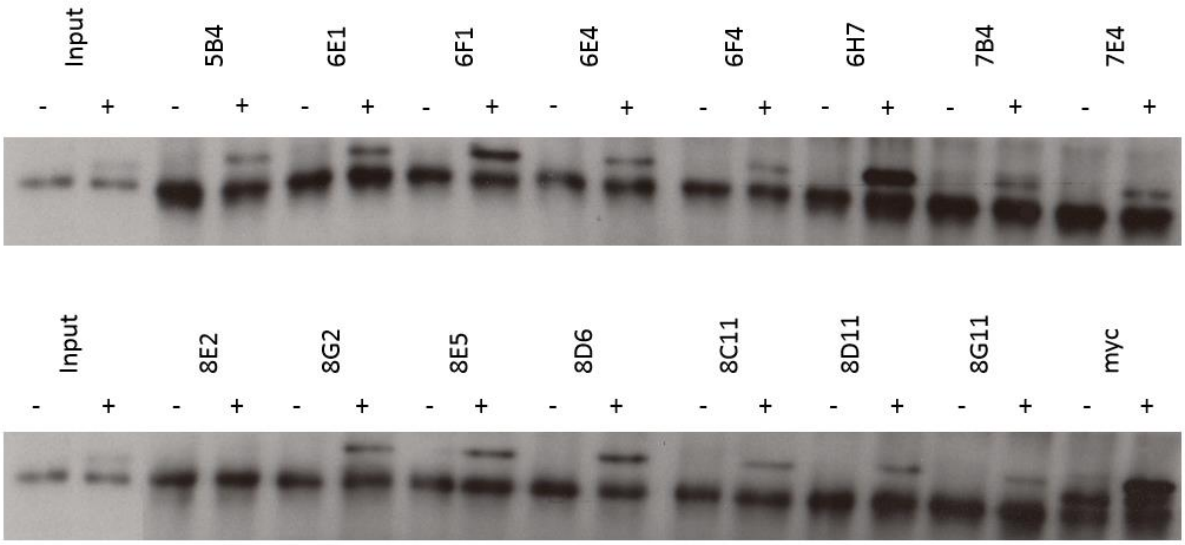

Figure 21: myc-IRF9 immunoprecipitation by antibodies derived from polyclonal hybridoma cultures. Fifteen candidates previously selected by western blot were tested on myc-IRF9 by immunoprecipitation. As an input (I), 50 µg of complete lysate was loaded. 1 mg of protein was used for immunoprecipitation. -: untransfected; +: transfected with myc-IRF9.

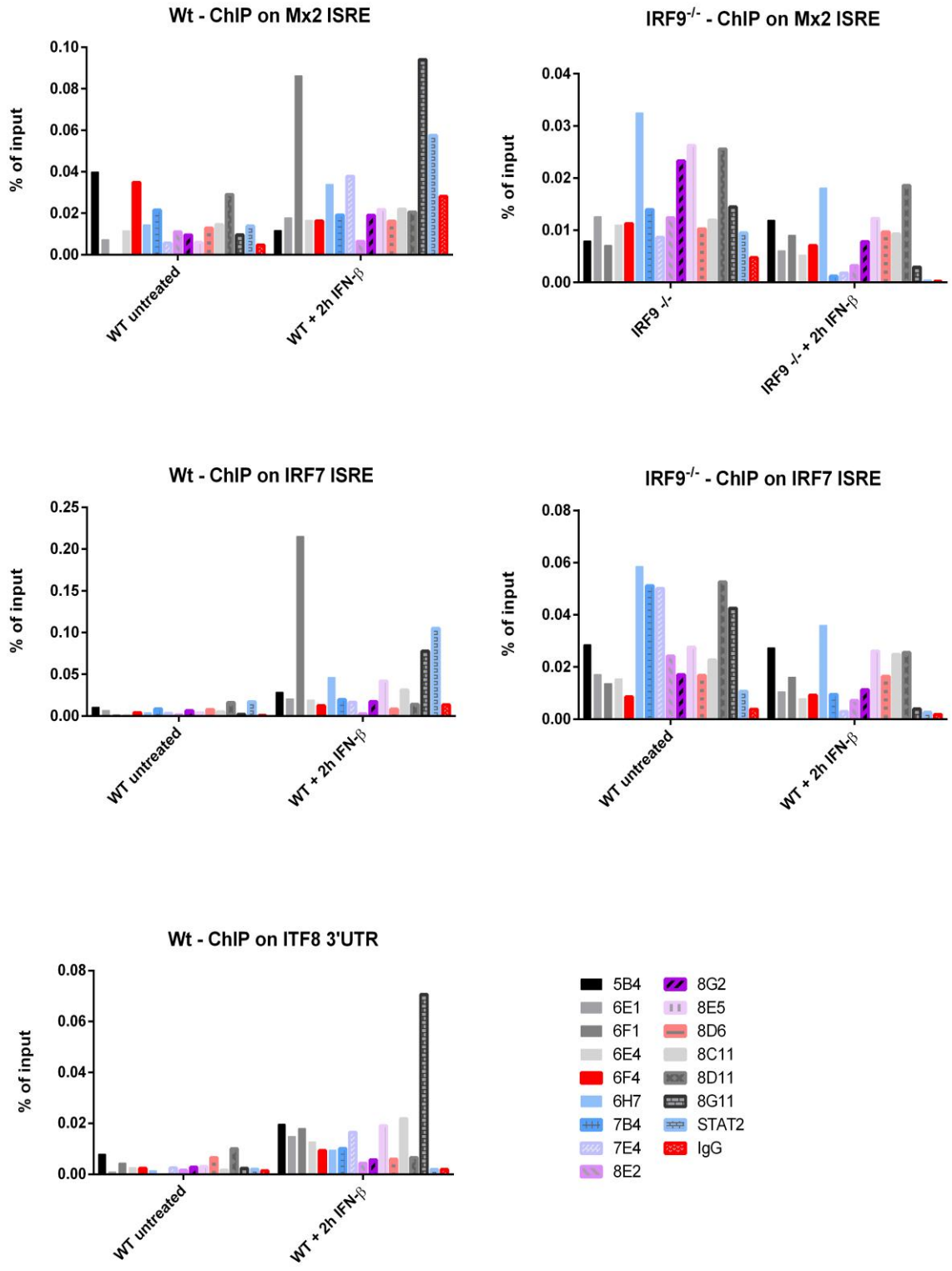

Figure 22: ChIP to test antibodies from polyclonal hybridoma cultures against ISRE-associated IRF9 in Wt BMDM and, as controls, IRF9-/- BMDM. The cells were treated with IFN-β for 2h. IRF9 was precipitated from the Mx2 and IRF7 gene ISRE using antibodies originating from the supernatant of polyclonal hybridoma cultures, STAT2 works as a positive control for the ISRE sites, whereas IgG functions as a negative control. An additional negative control is the recruitment of IRF9 to the 3'UTR of the IRF8 and IRF1 genes.

Discussion

The innate immune system represents the first line of defence against invading pathogens. Recognition of evolutionary conserved pathogen-associated molecular patterns (PAMP) by pattern recognition receptors (PRR) expressed on specialized cells of the innate immune system, initiates the innate immune response. Depending on the receptor and the nature of the PAMP, a variety of signaling cascades is activated, leading to the transcriptional activation of distinct genes regulating inflammation and innate host defence. However, the PRR do not necessarily act individually but also act in concert with each other [111-116]. Recently, the synergism between transcription factors at the endpoints of PRR and interferon pathways after *L. monocytogenes* infection has been described in our lab [96-98]. Unlike classical IFN-I-stimulated genes (ISGs) or NFκB target genes, transcriptional activation of the *Nos2* gene during infection with L. monocytogenes requires coordinate assembly of an initiation complex by the transcription factors NFκB and type I interferon-activated ISGF3. More precisely, NFκB and ISGF3 are involved in the recruitment of different portions of the mediator complex, the RNA polymerase II, pTEFb and TFIIH with their kinase subunit, as well as several other factors necessary for transcriptional activation of coregulated genes, like *Nos2* and *Il6*. Since *L. monocytogenes* has the ability to evade the phagolysosome, it is recognized by PRR at the cell surface and in the cytoplasm of infected cells, triggering both the NFκB pathway and the secretion of type I interferons. In order to study the mechanism of coregulation during an *L. monocytogenes* infection and to decipher the individual activities of NFκB and ISGF3, the input stimuli have to be examined separately. Treating BMDMs with heat-killed Listeria (hkL) only leads to the activation of NFκB, since hkL are captured in phagosomes and are unable to stimulate the cytoplasmic signaling pathways required for type I IFN production. Furthermore, the addition of IFN-β activates the interferon pathway and the assembly of the ISGF3 complex. Despite a difference in expression kinetics, simultaneous addition of hkL and IFN-β was shown to closely mimic the signaling of cells infected with *L. monocytogenes*, thus proving to be a valuable tool for the study of coregulated genes [96]. The question arose to what extent hkL activates the NFκB pathway via TNF production. First, the potential of hkL to activate NFκB was compared to TNF-α in RAW 264.7 cells, since their ability to produce TNF-α after LPS treatment and the expression of cell surface receptors should be comparable [103, 104]. However, RAW 264.7 remained unresponsive to TNF-α. This is an indication

that RAW 264.7 cells are unable to express the TNFAR or have a mutation in other components important for signaling, thus making them unresponsive to the cytokine. Indeed, leukemic and immortalized cells have often undergone significant mutations to become immortal, making it reasonable to believe that the biology of the cell could have been altered [117]. The effect of hkL and TNF-α as well as their respective double-treatment with IFN-β was therefore tested on BMDMs. Both double-treatments show a similar expression pattern on coregulated genes, even though the induction rates differ. Possibly, the activation kinetics or signal strength of the TNFAR alone differs from that caused by TNFAR and PRRs together in the case of hkL. TLR known to recognize Listeria PAMPS include TLR2 and TLR10 [118]. Furthermore, the simultaneous activation of different TLR was shown to synergize to increase the downstream gene expression [114]. For example, TLR2 and NOD2 or TLR5 and NOD2, all involved in the recognition of *L. monocytogenes,* act as synergistic combinations. However, NOD2 is a cytoplasmic PRR and should not be involved in the recognition of hkL, since it cannot evade the phagosome. TLR5 is activated by *L. monocytogenes* flagellin [119]. On the other hand, some L. m*onocytogenes* strains do not express flagellin at 37°C and we do not know if hkL contains flagellin, making the role of TLR5 in recognition of *L. monocytogenes* and hkL unclear [120]. Alternatively, it is possible that the recognition of hkL could activate additional pathways that increase Nos2 expression. A prominent target for this hypothesis would be MAP kinase pathways, since they are additional downstream targets of surface PRRs. However, pharmacological inhibition targeting ERK, JNK and p38MAPK did not show any significant reduction of *L. monocytogenes* induced *Nos2* expression [96]. Despite the fact that the reasons for the differences in the induction rates of coregulated genes after hkL or TNF-α treatment are still hypothetical, treating cells with either hkL or TNF together with IFN-β to mimic an infection with *L. monocytogenes* and separate the NFκB and type I IFN pathways, has been confirmed to be a valuable tool to study coregulated genes, such as *Nos2*.

The NFκB- and ISGF3-dependent coordinated assembly of the PIC on the *Nos2* promoter has also been studied by treating BMDMs with hkL and IFN-β. Most importantly for the second part of the thesis, TFIIH/CDK7 was shown to be recruited to the promoter after hkL treatment, but not after IFN-β. This suggest NFκB-dependent recruitment of TFIIH/CDK7 to provide Ser5 kinase activity for the RNA polymerase II CTD [96]. To find out if the NFκB-dependent recruitment of TFIIH/CDK7 is the result

of a direct interaction between p65 and CDK7, overexpressed p65 and CDK7 have been immunoprecipitated and interacting proteins were analysed by western blot. CDK7 and p65 were co-immunoprecipitated, indicating that the NFκB-dependent recruitment of TFIIH/CDK7 is indeed the result of a direct interaction. However, in a previous study from our lab it was shown that treatment with hkL alone also stimulated the recruitment of Brd4 to the promoter and Brd4 was shown to regulate the binding of TFIIH/CDK7 [97]. This result suggests an alternative mode of CDK7 recruitment via NFκB and Brd4. The co-immunoprecipitation of p65 and CDK7 cannot rule out the possibility that the interaction is dependent on Brd4. Nonetheless, p65 and CDK7 have been overexpressed, increasing their abundance within the cell compared to Brd4, which makes the interaction unlikely to be dependent on Brd4. It should also be noted that the initial recruitment of CDK7 via NFκB is Brd4-independent. This suggests the possibility that CDK7 recruitment may be both by direct NFκB interaction and by indirect interaction through Brd4 [97]. The elucidation of this question needs further investigation. In addition, p65 and IRF9 have also been co-immunoprecipitated. This interaction was unexpected and was originally regarded as a negative control for the co-immunoprecipitation. Although being unexpected, the interaction has already been shown *in vitro* with a GST pull-down assay [57]. However, the experiment has some limitations. First, due to time constraints this result was not reproduced, which makes it only preliminary. Next, the experiment lacks a proper negative control in two out of three cases, since p65 and IRF9 showed to be interaction partners. Additionally, it appears that there have been spill-overs to different neighbouring lanes, since some bands are continuous between two lanes. Despite these limitations, the results, together with the existing literature, indicate an interaction of p65 with both CDK7 and IRF9, but need to be repeated and confirmed with an endogenous IP. The study showing the interaction between p65 and IRF9, also revealed interactions of p65 with other members of the IRF family. More precisely, IRF2 was demonstrated to interact with p65 to inhibit NFκB-induced expression [57]. Even though IRF9 did not seem to affect NFκB-induced expression in a luciferase assay, the interaction between p65 and IRF9 could suggest an alternative mode of synergy between the NFκB and the interferon pathways.

IRF9 is widely employed for the regulation of IFN-responsive genes, both as a constituent of the canonical ISGF3 complex as well as a subunit of noncanonical STST/IRF9 complexes [44-48, 50-52]. Most recently, a study from our lab proposed

an important role for IRF9 as a component of non-canonical STAT complexes in the development of colitis [52]. In this case, IRF9 functions in a transcriptional complex with STAT1 during IFN-γ signaling and is necessary for the expression of the chemokine CXCL10. In order to investigate IRF9 regulation as well as DNA-dependent functions of IRF9, the need for an IRF9-specific antibody arose, since none of the commercially available antibodies was suitable for western blot or ChIP. In cooperation with Egon Ogris' lab, an IRF9-specific monoclonal antibody was generated. Polyclonal antibodies from mouse sera, polyclonal antibodies from polyclonal hybridoma cultures and finally monoclonal antibodies were tested in western blot for the detection of overexpressed and endogenous IRF9, in immunoprecipitation (IP) and in ChIP. At each step the most suitable mouse serum, polyconal hybridoma culture, or monoclonal hybridoma culture was selected for further applications.

Taken together, this thesis has confirmed that the treatment of cells with TNF and IFN-β is indeed a valuable tool to separate the NFκB and the type I IFN pathways to mimic gene coregulation as it occurs during *L. monocytogenes* infection. Additionally, the work that has been done here provides further indications how NFκB recruits the transcription factor TFIIH and its kinase subunit CDK7 to the *Nos2* promoter. Although, these results need to be confirmed, it seems that this recruitment is the result of a direct interaction between p65 and CDK7. Finally, a murine monoclonal IRF9 antibody has been generated, which is suitable for western blot and ChIP analysis.

To better understand the function of IRF9 during IFN-g signalling, ChIP-seq experiments are planned, using the generated monoclonal antibody. Furthermore, the identification of IRF9-dependent genes after IFN-γ treatment using RNA-sequencing will give us a better understanding of the proteins' function. Another point of interest is the identification of transient protein-protein and protein-DNA interactions of IRF9 and p65 using the recently described BioID method to gain a better understanding of the transcription factor protein networks controlling gene expression after NFκB and ISGF3 activation by infection with *L. monocytogenes* [121].

References

[1] Abul K. Abba, Andrew H. Lichtman, Shiv Pillai. Cellular and molecular immunology. 6th edition.

[2] Iwasaki A. and Medzhitov R. (2015). Control of adaptive immunity by the innate immune system. Nature Immunology 16, 343–353.

[3] Akira S., Uematsu S., Takeuchi O. (2006). Pathogen recognition and innate immunity. Cell 124:783–801.

[4] Kawai T, Akira S. (2009). The roles of TLRs, RLRs and NLRs in pathogen recognition. Int. Immunol. 21:317–337.

[5] Akira S., Takeda K. (2004). Toll-like receptor signaling. Nat. Rev. Immunol. 4:499–511.

[6] Kanneganti, T. D., Lamkanfi, M. and Nunez, G. (2007). Intracellular NOD-like receptors in host defense and disease. Immunity 27(4):549-559.

[7] Kobayashi, K.S., Chamaillard, M., Ogura, Y., Henegariu, O., Inohara, N., Nunez, G., and Flavell, R.A. (2005). Nod2-dependent regulation of innate and adaptive immunity in the intestinal tract. Science 307, 731–734.

[8] Mariathasan, S., Newton, K., Monack, D.M., Vucic, D., French, D.M., Lee, W.P., Roose-Girma, M., Erickson, S., and Dixit, V.M. (2004). Differential activation of the inflammasome by caspase-1 adaptors ASC and Ipaf. Nature 430, 213–218.

[9] Franchi, L., Munoz-Planillo, R., Nunez, G. Sensing and reacting to microbes through the inflammasomes. Nature Immunology 13(4):325-32 (2012).

[10] Kumar H., Kawai T., Akira S. (2011). Pathogen Recognition by the innate immune system. Int. Rev. Immunol., 30:16-34

[11] Loo Y.M., Gale M. Jr. (2011). Immune Signaling by RIG-I-like Receptors. Immunity 34:680-692.

[12] Satoh T., Kato H., Kumagai Y., Yoneyama M., Sato S., Matsushita K., Tsujimura T., Fujita T., Akira S., Takeuchi O. (2010). LGP2 is a positive regulator of RIG-I- and MDA5- mediated antiviral responses. Proc Natl. Acad Sci USA 107:1512-1517.

[13] Rothenfusser S., Goutagny N., DiPerna G., Gong M., Monks B.G., Schoenemeyer A., Yamamoto M., Akira S., Fitzgerald K.A. (2005). The RNA helicase LGP2 inhibits TLR-independent sensing of viral replication by Retinoic acid-inducible gene-I. J Immunol 175:2851-2858

[14] Kell A.M., Gale M. Jr (2015). RIG-I in RNA virus recognition. Virology 479-480:110-121

[15] Abdullah Z., Schlee M., Roth S., Mraheil M.A., Barchet W., Bottcher J., Hain T., Geiger S., Hayakawa Y., Fritz J.H., Civril F., Hopfner K.P., Kurts C., Ruland J., Hartmann G., Chakraborty T., Knolle P.A. (2012). RIG-I detects infection with live Listeria by sensing secreted bacterial nucleic acids. EMBO J 31:4153-4164

[16] Yoneyama M., Fujita T. (2008). Structural Mechanism of RNA Recognition by the RIG-I-like Receptors. Immunity 29:178-181

[17] Goubau D., Deddouche S. and Reis e Sousa C. (2013). Cytosolic Sensing of Viruses. Immunity 38:855-869

[18] Dixit E., Boulant S., Zhang Y., Lee A.S.Y., Odendall C., Shum B., Hacohen N., Chen Z.J., Whelan S.P., Fransen M., Nibert M.L., Superti-Furga G., Kagan J.C. (2010). Peroxisomes Are Signaling Platforms for Antiviral Innate Immunity. Cell 141: 669–682

[19] O'Neill, L.A. (2009). DNA makes RNA makes innate immunity. Cell 138, 428–430.

[20] Hemmi H., Takeuchi O., Kawai T., Kaisho T.,Sato S., Sanjo H., Matsumoto M., Hoshino K., Wagner H., Takeda K. and Akira S. (2000). A Toll-like receptor recognizes bacterial DNA. Nature 408, 740–745

[21] Barber G.N. (2014). STING-dependent cytosolic DNA sensing pathways. Trends Immunol. 35(2):88-93.

[22] Ishii K.J., Coban C., Kato H., Takahashi K., Torii Y., Takeshita F., Ludwig H., Sutter G., Suzuki K., Hemmi H., Sato S., Yamamoto M., Uematsu S., Kawai T., Takeuchi O. and Akira S. (2006). A Toll-like receptor-independent antiviral response induced by double-stranded B-form DNA. Nat. Immunol. 7, 40–48.

[23] Takaoka A., Wang Z., Choi M.K., Yanai H., Negishi H., Ban T., Lu Y., Miyagishi M., Kodama T., Honda K., Ohba Y., Taniguchi T. (2007). DAI (DLM-1/ZBP1) is a cytosolic DNA sensor and an activator of innate immune response. Nature 448(7152):501-5.

[24] Hornung V., Ablasser A., Charrel-Dennis M., Bauernfeind F., Horvath G., Caffrey D.R., Latz E., Fitzgerald K.A. (2009). AIM2 recognizes cytosolic dsDNA and forms a caspase-1-activating inflammasome with ASC. Nature 458(7237):514-8.

[25] Ishikawa H., Barber G.N. (2008). STING is an endoplasmic reticulum adaptor that facilitates innate immune signaling. Nature 455(7213):674-8.

[26] Ishikawa H., Barber G.N. (2009). STING regulates intracellular DNA-mediated, type I interferon-dependent innate immunity. Nature; 461, 788-792.

[27] Sun, L., Wu, J., Du, F., Chen, X., and Chen, Z.J. (2013). Cyclic GMP-AMP synthase is a cytosolic DNA sensor that activates the type I interferon pathway. Science 339, 786–791.

[28] Cai X., Chiu, Y.H., Chen Z.J. (2014). The cGAS-cGAMP-STING Pathway of Cytosolic DNA Sensing and Signaling. Mol Cell. 54(2):289-96.

[29] Keating S.E., Baran M., Bowie A.G. (2011). Cytosolic DNA sensors regulating type I interferon induction. Trends Immunol. 32:574-81.

[30] Zhang Z., Yuan B., Bao M., Lu N., Kim T., Liu Y.J. (2011). The helicase DDX41 senses intracellular DNA mediated by the adaptor STING in dendritic cells. Nat. Immunol. 12(10):959-965 (2011).

[31] Yan N. and Chen Z.J. Intrinsic antiviral immunity (2012). Nat. Immunol. 13, 214–222.

[32] Meyer O. (2009). Interferons and autoimmune disorders. Joint Bone Spine. 76(5):464-73.

[33] González-Navajas J.M., Lee J., David M., Raz E. (2012). Immunomodulatory functions of type I interferons. Nat Rev Immunol. 12(2):125-35.

[34] Rauch I, Müller M., Decker T. (2013). The regulation of inflammation by Interferons and their STATs. JAKSTAT 2(1):e23820.

[35] Pestka S., Krause C.D. and Walter M.R. (2004) Interferons, interferon-like cytokines, and their receptors. *Immunol. Rev.* 202, 8–32.

[36] Liu Y.J. (2005). IPC: professional type 1 interferon-producing cells and plasmacytoid dendritic cell precursors. *Annu. Rev. Immunol.* 23:275–306

[37] Schneider W.M., Chevillotte M.D., Rice C.M. (2014). Interferon-stimulated genes: a complex web of host defenses. Annu Rev Immunol. 32:513-45.

[38] Schroder K., Hertzog P.J., Ravasi T., Hume D.A. (2004). Interferon-gamma: an overview of signals, mechanisms and functions. J Leukoc Biol. 75(2):163-89.

[39] Levy D.E., Lew D.J., Decker T., Kessler D.S., and Darnell, Jr J.E. (1990). Synergistic interaction between interferon-alpha and interferon-gamma through induced synthesis of one subunit of the transcription factor ISGF3. EMBO J. 9(4): 1105–1111.

[40] Sommereyns C., Paul S., Staeheli P., Michiels T. (2008). IFN-lambda (IFN-*λ*) is expressed in a tissue-dependent fashion and primarily acts on epithelial cells in vivo. P*LoS Pathog.* 4:e1000017

[41] Darnell J.E. Jr, Kerr I.M. and Stark G.R. (1994). Jak-STAT pathways and transcriptional activation in response to IFNs and other extracellular signaling proteins. Science 264(5164):1415-21.

[42] Schindler C., Levy D.E. and Decker T. (2007) JAK-STAT signaling: from interferons to cytokines. J Biol Chem. 282(28):20059-63.

[43] Au-Yeung N., Mandhana R., Horvath C.M. (2013). Transcriptional regulation by STAT1 and STAT2 in the interferon JAK-STAT pathway. JAKSTAT 2(3):e23931.

[44] Perry S.T., Buck M.D., Lada S.M., Schindler C., Shresta S. (2011). STAT2 mediates innate immunity to Dengue virus in the absence of STAT1 via the type I interferon receptor. PLoS Pathog 7:e1001297.

[45] Fink, K., Martin, L., Mukawera, E., Chartier, S., De Deken, X., Brochiero, E., Miot, F. and Grandvaux, N. (2013). IFN beta/TNF alpha synergism induces a non-canonical STAT2/IRF9-dependent pathway triggering a novel DUOX2 NADPH Oxidase-mediated airway antiviral response. Cell Research *23*, 673–690.

[46] Abdul-Sater A.A., Majoros A., Plumlee C.R., Perry S., Gu A.D., Lee C., Shresta S., Decker T., Schindler C. (2015). Different STAT Transcription Complexes Drive Early and Delayed Responses to Type I IFNs. J Immunol. 195(1):210-6.

[47] Fink K., Grandvaux N. (2013). STAT2 and IRF9: beyond ISGF3. JAKSTAT 2:e27521.

[48] Cheon H., Stark G.R. (2009). Unphosphorylated STAT1 prolongs the expression of interferon-induced immune regulatory genes. Proc Natl Acad Sci USA 106:9373–9378.

[49] Decker T., Kovarik P., Meinke A. (1997). GAS elements: a few nucleotides with a major impact on cytokine-induced gene expression. J Interferon Cytokine Res. 17(3):121-34.

[50] Majumder S., Zhou L.Z., Chaturvedi P., Babcock G., Aras S., Ransohoff R.M. (1998). p48/STAT-1alpha-containing complexes play a predominant role in induction of IFN-gamma-inducible protein, 10 kDa (IP-10) by IFN-gamma alone or in synergy with TNF-alpha. J Immunol 161:4736–4744.

[51] Morrow A.N., Schmeisser H., Tsuno T., Zoon K.C. (2011). A novel role for IFN-stimulated gene factor 3II in IFN-_ signaling and induction of antiviral activity in human cells. J Immunol 186:1685–1693.

[52] Rauch I., Rosebrock F., Hainzl E., Heider S., Majoros A., Wienerroither S., Strobl B., Stockinger S., Kenner L., Müller M., Decker T. (2015). Noncanonical Effects of IRF9 in Intestinal Inflammation: More than Type I and Type III Interferons. Mol Cell Biol. 35(13):2332-43.

[53] Zhang X.J., Jiang D.S., Li H. (2014). The interferon regulatory factors as novel potential targets in the treatment of cardiovascular diseases. Br J Pharmacol.

[54] Jiang D.S., Luo Y.X., Zhang R., Zhang X.D., Chen H.Z., Zhang Y., Chen K., Zhang S.M., Fan G.C., Liu P.P., Liu D.P., Li H. (2014). Interferon regulatory factor 9 protects against cardiac hypertrophy by targeting myocardin. Hypertension. 63(1):119-27.

[55] Zhang Y., Liu X., She Z.G., Jiang D.S., Wan N., Xia H., Zhu X.H., Wei X., Zhang X.D., Li H. (2014). Interferon regulatory factor 9 is an essential mediator of heart dysfunction and cell death following myocardial ischemia/reperfusion injury. Basic Res Cardiol. 109(5):434.

[56] Chen H.Z., Guo S., Li Z.Z., Lu Y., Jiang D.S., Zhang R., Lei H., Gao L., Zhang X., Zhang Y., Wang L., Zhu L.H., Xiang M., Zhou Y., Wan Q., Dong H., Liu D.P., Li H. (2014). A critical role for interferon regulatory factor 9 in cerebral ischemic stroke. J Neurosci. 34(36):11897-912.

[57] Drew P.D., Franzoso G., Carlson L.M., Biddison W.E., Siebenlist U., Ozato K. (1995). Interferon regulatory factor-2 physically interacts with NF-kappa B *in vitro* and inhibits NF-kappa B induction of major histocompatibility class I and beta 2-microglobulin gene expression in transfected human neuroblastoma cells. J Neuroimmunol 63: 157–162.

[58] Zhang S.M., Zhu L.H., Chen H.Z., Zhang R., Zhang P., Jiang D.S., Gao L., Tian S., Wang L., Zhang Y., Wang P.X., Zhang X.F., Zhang X.D., Liu D.P., Li H. (2014). Interferon regulatory factor 9 is critical for neointima formation following vascular injury. Nat Commun. 6:6882.

[59] Wang X.A., Zhang R., Jiang D., Deng W., Zhang S., Deng S., Zhong J., Wang T., Zhu L.H., Yang L., Hong S., Guo S., Chen K., Zhang X.F., She Z., Chen Y., Yang Q., Zhang X.D., Li H. (2013). Interferon regulatory factor 9 protects against hepatic insulin resistance and steatosis in male mice. Hepatology. 58(2):603-16.

[60] Hayden, M. S., & Ghosh, S. (2011). NF-κB in immunobiology. Cell Research, 1(2), 223–244.

[61] Hayden M.S. and Gosh S. (2014). Regulation of NF-κB by TNF family cytokines. Semin Immunol. 26(3):253-66.

[62] Chen Z., Hagler J., Palombella V.J., Melandri F., Scherer D., Ballard D., Maniatis T. (1995). Signal-induced site-specific phosphorylation targets I kappa B alpha to the ubiquitin-proteasome pathway. Genes Dev 9:1586–97.

[63] Brasier, A.R., Tian, B., Jamaluddin, M., Kalita, M.K., Garofalo, R.P., and Lu, M. (2011). RelA Ser276 phosphorylation-coupled Lys310 acetylation controls transcriptional elongation of inflammatory cytokines in respiratory syncytial virus infection. Journal of Virology 85, 11752–11769.

[64] Oeckinghaus, A., and Ghosh, S. (2009) The NF-B family of transcription factors and its regulation. Cold Spring Harb. Perspect. Biol. 1,a000034

[65] Wong E.T., Tergaonkar V. (2009). Roles of NF-kappaB in health and disease: mechanisms and therapeutic potential. Clin Sci (Lond). 116(6):451-65.

[66] Gerondakis S., Fulford T.S., Messina N.L., Grumont R.J. (2014). NF-κB control of T cell development. Nat. Rev. Immunol.15, 15–25.

[67] Hahn S. (2004). Structure and mechanism of the RNA polymerase II transcription machinery. Nat Struct Mol Biol. 11(5):394-403.

[68] Phatnani H.P., Greenleaf A.L. (2006). Phosphorylation and functions of the RNA polymerase II CTD. Genes Dev. 20(21):2922-36.

[69] Hsin J.P., Manley J.L. (2012). The RNA polymerase II CTD coordinates transcription and RNA processing. Genes Dev. 26(19):2119-37.

[70] Nechaev S., and Adelman K. (2011). Pol II waiting in the starting gates: Regulating the transition from transcription initiation into productive elongation. Biochim Biophys Acta. 1809(1):34-45.

[71] Egloff S., Murphy S. (2008). Cracking the RNA polymerase II CTD code. Trends Genet. 24(6):280-8.

[72] Yamaguchi Y., Takagi T., Wada T., Yano K., Furuya A., Sugimoto S., Hasegawa J., Handa H. (1999). NELF, a multisubunit complex containing RD, cooperates with DSIF to repress RNA polymerase II elongation. Cell 97: 41–51.

[73] Wu C.H., Yamaguchi Y., Benjamin L.R., Horvat-Gordon M., Washinsky J., Enerly E., Larsson J., Lambertsson A., Handa H., Gilmour D. (2003). NELF and DSIF cause promoter proximal pausing on the hsp70 promoter in Drosophila. Genes Dev 17: 1402–1414.

[74] Spain M.M., Govind C.K. (2011). A role for phosphorylated Pol II CTD in modulating transcription coupled histone dynamics. Transcription 2: 78–81.

[75] Glover-Cutter K., Larochelle S., Erickson B., Zhang C., Shokat K., Fisher R.P., and Bentley D.L. (2009). TFIIH-Associated Cdk7 Kinase Functions in Phosphorylation of C-Terminal Domain Ser7 Residues, Promoter-Proximal Pausing, and Termination by RNA polymerase II. Molecular and Cellular Biology *29*, 5455–5464.

[76] Hsin J.P., Sheth A., Manley J.L. (2011). RNAP II CTD phosphorylated on threonine-4 is required for histone mRNA 39 end processing. Science 334: 683–686.

[77] Egloff S., O'Reilly D., Chapman R.D., Taylor A., Tanzhaus K., Pitts L., Eick D., Murphy S. (2007). Serine-7 of the RNA polymerase II CTD is specifically required for snRNA gene expression. Science 318(5857):1777-9.

[78] Egloff S., Dienstbier M., and Murphy S. (2012). Updating the RNA polymerase CTD code: adding gene-specific layers. Trends in Genetics *28*, 333–341.

[79] Disson O, et al. (2008) Conjugated action of two species-specific invasion proteins for fetoplacental listeriosis. Nature 455:1114–1118

[80] Cossart P. (2011). Illuminating the landscape of host-pathogen interactions with the bacterium Listeria monocytogenes. Proc Natl Acad Sci U S A. 108(49):19484-91.

[81] Freitag N.E., Port G.C., Miner M.D. (2009). Listeria monocytogenes - from saprophyte to intracellular pathogen. Nat Rev Microbiol. 7(9):623-8.

[82] Lambrechts, A., Gevaert, K., Cossart, P., Vandekerckhove, J., and Van Troys, M. (2008). Listeria comet tails: the actin-based motility machinery at work. Trends Cell Biol 18, 220–227.

[83] Sauer J.D., Sotelo-Troha K., von Moltke J., Monroe K.M., Rae C.S., Brubaker S.W., Hyodo M., Hayakawa Y., Woodward J.J., Portnoy D.A., Vance R.E. (2011). The N-ethyl-N-nitrosourea-induced Goldenticket mouse mutant reveals an essential function of Sting in the in vivo interferon response to Listeria monocytogenes and cyclic dinucleotides. Infect Immun. 79(2):688-94.

[84] Jin L., Getahun A., Knowles H.M., Mogan J., Akerlund L.J., Packard T.A., Perraud A.L., Cambier J.C. (2013). STING/MPYS mediates host defence against Listeria monocytogenes infection by regulating Ly6C(hi) monocyte migration. J Immunol. 190(6):2835-43.

[85] Bogdan, C. (2001). Nitric oxide and the immune response. Nat Immunol. 2(10):907-16.

[86] Zwaferink H., Stockinger S., Reipert S., Decker T. (2008). Stimulation of inducible nitric oxide synthase expression by beta interferon increases necrotic death of macrophages upon Listeria monocytogenes infection. Infect Immun. 76(4):1649-56.

[87] Lechner M., Lirk P., Rieder J.. (2005). Inducible nitric oxide synthase (iNOS) in tumor biology: the two sides of the same coin. Semin Cancer Biol. 15(4):277-89.

[88] MacMicking J.D., Nathan C., Hom G., Chartrain N., Fletcher D.S., Trumbauer M., Stevens K., Xie Q.W., Sokol K., Hutchinson N., Chen H., Mudget J.S. (1995). Altered responses to bacterial infection and endotoxic shock in mice lacking inducible nitric oxide synthase. Cell 19;81(4):641-50.

[89] Shiloh M.U., MacMicking J.D., Nicholson S., Brause J.E., Potter S., Marino M., Fang F., Dinauer M., Nathan C. (1999). Phenotype of mice and macrophages deficient in both phagocyte oxidase and inducible nitric oxide synthase. Immunity 10(1):29-38.

[90] Cole, C., Thomas, S., Filak, H., Henson, P.M., and Lenz, L.L. (2012). Nitric Oxide Increases Susceptibility of Toll-like Receptor-Activated Macrophages to Spreading Listeria monocytogenes. Immunity *36*, 807–820.

[91] Kamijo, R., Harada, H., Matsuyama, T., Bosland, M., Gerecitano, J., Shapiro, D., Le, J., Koh, S.I., Kimura, T., and Green, S.J. (1994). Requirement for transcription factor IRF-1 in NO synthase induction in macrophages. Science *263*, 1612–1615.

[92] Meraz, M.A., White, J.M., Sheehan, K., and Bach, E.A. (1996). Targeted Disruption of the Stat1 Gene in Mice Reveals Unexpected Physiologic Specificity in the JAK–STAT Signaling Pathway. Cell 84(3):431-42.

[93] Xie, Q.W. (1993). Promoter of the mouse gene encoding calcium-independent nitric oxide synthase confers inducibility by interferon gamma and bacterial lipopolysaccharide. J Exp Med *177*, 1779–1784.

[94] Gao J.J.J., Filla M.B.M., Fultz M.J.M., Vogel S.N.S., Russell S.W.S., Murphy, W.J.W. (1998). Autocrine/paracrine IFN-alphabeta mediates the lipopolysaccharide-induced activation of transcription factor Stat1alpha in mouse macrophages: pivotal role of Stat1alpha in induction of the inducible nitric oxide synthase gene. J Immunol. *161*, 4803–4810.

[95] Stockinger S., Reutterer B., Schaljo B., Schellack C., Brunner S., Materna T., Yamamoto M., Akira S., Taniguchi T., Murray P.J., Müller M., Decker T. (2004). IFN regulatory factor 3-dependent induction of type I IFNs by intracellular bacteria is mediated by a TLR- and Nod2-independent mechanism. J Immunol. 173(12):7416-25.

[96] Farlik M., Reutterer B., Schindler C., Greten F., Vogl C., Müller M., and Decker T. (2010). Nonconventional Initiation Complex Assembly by STAT and NFκB Transcription Factors Regulates Nitric Oxide Synthase Expression. Immunity 33, 25–34.

[97] Wienerroither S., Rauch I., Rosebrock F., Jamieson A.M., Bradner J., Muhar M., Zuber J., Müller M., Decker T. (2014). Regulation of NO synthesis, local inflammation, and innate immunity to pathogens by BET family proteins. Mol Cell Biol. 34(3):415-27.

[98] Wienerroither S., Shukla P., Farlik M., Majoros A., Stych B., Vogl C., Cheon H., Stark G.R., Strobl B., Müller M., Decker T. (2015). Cooperative Transcriptional Activation of Antimicrobial Genes by STAT and NF-κB Pathways by Concerted Recruitment of the Mediator Complex. Cell Rep. 12(2):300-12.

[99] Kimura T., Kadokawa Y., Harada H., Matsumoto M., Sato M., Kashiwazaki Y., Tarutani M., Tan R.S., Takasugi T., Matsuyama T., Mak T.W., Noguchi S., Taniguchi T. (1996). Essential and non-redundant roles of p48 (ISGF3 gamma) and IRF-1 in both type I and type II interferon responses, as revealed by gene targeting studies. Genes Cells 1:115–124.

[100] Baccarini M., Bistoni F., Lohmann Matthes M.L. (1985). In vitro natural cell-mediated cytotoxicity against *Candida albicans*: macrophage precursors as effector cells. J. Immunol. 134:2658–2665.

[101] Graham F.L., Smiley J., Russell W.C., Nairn R. (1977). Characteristics of a human cell line transformed by DNA from human adenovirus type 5. J. Gen. Virol. 36 (1): 59–74.

[102] Yang J., Richmond A.J. (2009). Monitoring NF-kappaB mediated chemokine transcription in tumorigenesis. Methods in Enzymology 460:347-55.

[103] Berghausa L. J., Moorea J. N., Hurleya D. J., Vandenplasa M. L., Fortesa B. P., Wolfert M. A., Boons G. J. (2009). Innate immune responses of primary murine macrophage-lineage cells and RAW 264.7 cells to ligands of Toll-like receptors 2, 3, and 4. Comparative Immunology, Microbiology and Infectious Diseases 33, Issue 5, 443–454.

[104] Lichtman S.N., Wang J., Lemasters J.J. (1998). LPS receptor CD14 participates in release of TNF-α in RAW 264.7 and peritoneal cells but not in Kupffer cells. American Journal of Physiology - Gastrointestinal and Liver Physiology 275, no. 1, G39-G46.

[105] O'Riordan M., Gonzales C.H. Yi R., Lee K.D., Portnoy D.A. (2002). Innate recognition of bacteria by a macrophage cytosolic surveillance pathway. Proc. Natl. Acad. Sci. USA 99: 13861–13866.

[106] Opitz B., Püschel A., Beermann W., Hocke A.C., Förster S., Schmeck B., van Laak V., Chakraborty T., Suttorp N., Hippenstiel S. (2006). Listeria monocytogenes activated p38 MAPK and induced IL-8 secretion in a nucleotide-binding oligomerization domain 1-dependent manner in endothelial cells. J Immunol 176:484-490.

[107] Nygren P.A., Stahl S., M. Uhlen (1994). Engineering proteins to facilitate bioprocessing. Trends Biotechnol, 12, 184–188.

[108] Fox, J. D. and Waugh, D. S. (2003). Maltose-binding protein as a solubility enhancer. Methods Mol. Biol. 205: 99-117.

[109] Weihua X., Kolla V., Kalvakolanu D.V. (1997). Interferon γ-induced transcription of the murine ISGF3γ (p48) gene is mediated by novel factors. Proc Natl Acad Sci U S A. 94(1): 103–108.

[110] Nanus D.M., Geng Y., Shen R., Lai H.K., Pfeffer S.R., Pfeffer L.M. (2000). Interaction of retinoic acid and interferon in renal cancer cell lines. J Interferon Cytokine Res. 20(9):787-94.

[111] Bagchi A., Herrup E.A., Warren H.S., Trigilio J., Shin H.S., Valentine C., Hellman J. (2007). MyD88-dependent and MyD88-independent pathways in synergy, priming, and tolerance between TLR agonists. J. Immunol. 178: 1164– 1171.

[112] Watanabe T., Kitani A., Murray P.J., Strober W. (2004). NOD2 is a negative regulator of Toll-like receptor 2-mediated T helper type 1 responses. Nat. Immunol. 5: 800– 808.

[113] Zhu Q., Egelston C., Vivekanandhan A., Uematsu S., Akira S., Klinman D.M., Belyakov I.M., Berzofsky J.A. (2008). Toll-like receptor ligands synergize through distinct dendritic cell pathways to induce T cell responses: implications for vaccines. Proc. Natl. Acad. Sci. U. S. A. 105: 16260– 16265.

[114] Timmermans K., Plantinga T.S., Kox M., Vaneker M., Scheffer G.J., Adema G.J., Joosten L.A., Netea MG. (2013). Blueprints of signaling interactions between pattern recognition receptors: implications for the design of vaccine adjuvants. Clin Vaccine Immunol. 20(3):427-32.

[115] Hu X., Chen J., Wang L., Ivashkiv L.B. (2007). Crosstalk among Jak-STAT, Toll-like receptor, and ITAM-dependent pathways in macrophage activation. J Leukoc Biol. 82(2):237-43.

[116] Oeckinghaus A., Hayden M.S., Ghosh S. (2011). Crosstalk in NF-κB signaling pathways. Nat Immunol. 12(8):695-708

[117] Maqsood, I.M., Matin M.M., Bahrami A.R.; Ghasroldasht M.M. (2013). "Immortality of cell lines: Challenges and advantages of establishment". Cell Biology International 37 (10): 1038–45.

[118] Regan T., MacSharry J., Brint E. (2014). Tracing innate immune defences along the path of Listeria monocytogenes infection. Immunol Cell Biol. 92(7):563-9.

[119] Hayashi F., Smith K.D., Ozinsky A., Hawn T.R., Yi E.C., Goodlett D.R., Eng J.K., Akira S., Underhill D.M., Aderem A. (2001). The innate immune response to bacterial flagellin is mediated by Toll-like receptor 5. Nature 410, 1099–110310.

[120] Way S.S., Thompson L.J., Lopes J.E., Hajjar A.M., Kollmann T.R., Freitag N.E., Wilson C.B. (2004). Characterization of flagellin expression and its role in *Listeria monocytogenes* infection and immunity. Cell. Microbiol. 6, 235–242

[121] Roux K.J., Kim D.I., Burke B. (2013). BioID: a screen for protein-protein interactions. Curr Protoc Protein Sci. 74:Unit 19.23.

„Ich habe mich bemüht, sämtliche Inhaber der Bildrechte ausfindig zu machen und ihre Zustimmung zur Verwendung der Bilder in dieser Arbeit eingeholt. Sollte dennoch eine Urheberrechtsverletzung bekannt werden, ersuche ich um Meldung bei mir.“

Appendix

Primers

Cloning into pGEX4T1

p65 for EcoRI	5’-GATGAATTCATGGACGATCTGTTTCCCC-3’
p65 rev XhoI	5’-GATCTCGAGACTTAGGAGCTGATCTGACTCA-3’
CDK7 for BamHI	5’-GATGGATCCATGGCTGTGGACGTGAAG-3’
CDK7 rev EcoRI	5’-GATGAATTCCTAAAAAATGAGCTTCTTGGGC-3

Cloning into pET23a+

IRF9 for NheI	5’-GATGCTAGCATGCACCTCCCCGGAGG-3’
IRF9 rev XhoI	5’-GATCTCGAGGTGTCCCAGAGCAGAGGG-3’

Cloning into pET-Duet1

IRF9 for EcoRI	5’- GATGAATTCGATGCACCTCCCCGGAGG-3’
IRF9 rev HindIII	5’- GATAAGCTTTCAGTGTCCCAGAGCAGA-3’

Cloning into pCMV

p65 for EcoRI	5’-GATGAATTCTGATGGACGATCTGTTTCCCC-3’
p65 rev XhoI	5’-GATCTCGAGACTTAGGAGCTGATCTGACTCA-3’
IRF9 for EcoRI	5’-GATGAATTCTGATGCACCTCCCCGGAGG-3’
IRF9 rev XhoI	5’-GATCTCGAGTCAGTGTCCCAGAGCAGA-3’
p50 for EcoRI	5’-GATGAATTCTGATGGCAGACGATGATCCCTAC-3’
p50 rev XhoI	5’-GATCTCGAGTTAGCCATGGGTGACCCCTGC-3’
cycH for XhoI	5’-GATCTCGAGTGATGTATCACAGCAGCAGCCA-3’
cycH rev NotI	5’-GATGCGGCCGCTTAGAGAGAATCTACCAGGTC-3’

Gateway Cloning

CDK7 for	5’-GGGGACAAGTTTGTACAAAAAAGCAGGCTTCATGGC TGTGGACGTGAAGTCTCGA-3’
CDK7 rev	5’-GGGGACCACTTTGTACAAGAAAGCTGGGTCCTACTAAA AAATGAGCTTCTTGGGCAAT-3’

qPCR primers

Nos2 for	5’-CAATGGGCAGGTATGCTGTGTTTG
Nos2 rev	5’-GTTTGTACAGCCCAGCTGCGGAA
IL-6 for	5’-CTGCAAGAGACTTCCATCCAG
IL-6 rev	5’-AGTGGTATAGACAGGTCTGTTGG
IκB-α for	5’-ACGGAGTCAGAATTCACAGAGG
IκB-α rev	5’-CCGAATCACCCCAGTAAAATG
Mx1 for	5’-GACTACCACTGAGATGACCCAGC
Mx1 rev	5’-ATTTCCTCCCCAAATGTTTTCA
Mx2 for	5’-CCAGTTCCTCTCAGTCCCAAGATT
Mx2 rev	5’-TACTGGATGATCAAGGGAACGTGG
GAPDH for	5’-CATGGCCTTCCGTGTTCCTA
GAPDH rev	5’-GCGGCACGTCAGATCCA

Antibodies

Pol II	Santa Cruz (Cat.No. sc-899)
CDK7	Santa Cruz (Cat.No. sc-529)
p65 NFκB	Santa Cruz (Cat.No. sc-372)
STAT1	Cell Signaling (Cat.No. #4597)
Myc-tag	Cell Signaling (Cat.No. #2276; Clone 9B11)
HA-tag	Biolegend (Cat.No. MMS-101P; Clone 16B12)
6xHis-tag	GE Healthcare (Cat.No. 27-4710-01)
GST-tag	was provided by the Martens Lab

Abstract

The innate immune system represents the first line of defence against invading pathogens. Recognition of evolutionary conserved pathogen-associated molecular patterns (PAMP) by pattern recognition receptors (PRR) expressed on specialized cells of the innate immune system, initiates the innate immune response. Depending on the receptor and the nature of PAMP, a variety of signaling cascades are activated, leading to the transcriptional activation of distinct genes regulating inflammation and innate host defence. *Listeria monocytogenes* is a facultative intracellular pathogen able to evade the phagosome into the cytoplasm, where it replicates. *L. monocytogenes* is first sensed by PRR at the cell surface, which activates the nuclear factor κB (NFκB) pathway to induce the expression of inflammatory genes. After phagosomal evasion, the pathogen is recognized by cytosolic sensors, which induce the interferon response factor 3 (IRF3) -dependent expression and secretion of type I Interferons (IFN). In turn, type I interferons bind the IFN-α receptor (IFNAR) to further activate the Janus kinase/signal transducers and activators of transcription (JAK/STAT) signaling pathway, resulting in the assembly of the interferon-stimulated gene factor 3 (ISGF3) complex and thus to the expression of interferon stimulated genes (ISGs). Here we generate and characterize a monoclonal antibody against one of the ISGF3 subunits, IRF9. We demonstrate that this antibody is a valuable tool to study the ISGF3 interaction with chromatin.

Unlike classical NFκB- or IFN-dependent genes, coregulated genes, including the gene coding for the Nitric oxide synthase 2 (*Nos2*), need a coordinated assembly of the transcription machinery dependent on both NFκB and ISGF3. Treating bone marrow derived macrophages (BMDMs) with heat-killed Listeria (hkL) and IFN-β, activates the NFκB and the IFN pathway respectively, mimicking the signaling profile of macrophages infected with *L. monocytogenes*. Here we demonstrate the feasibility of this approach for studying the transcriptional activation of coregulated genes. Both hkL and the classical NFκB activator, tumor necrosis factor α (TNF-α) synergized with type I IFN in stimulating expression of coregulated genes, although hkL generated higher induction rates compared to TNF-α.

Recruitment of the general transcription factor TFIIH and its kinase subunit CDK7 (cyclin-dependant kinase 7) to the *Nos2* promoter during transcriptional activation is dependent on NFκB, hence hkL alone is sufficient to enrich TFIIH/CDK7 at the DNA.

In the course of this thesis, CDK7 and p65 were co-immunoprecipitated after overexpression in HEK293 cells. Although needing further investigation, this is an indication that the recruitment of TFIIH/CDK7 to the *Nos2* promoter is the result of a direct interaction between NFκB p65 and CDK7. Although the implications of this interaction are unclear, IRF9 was also co-immunoprecipitated with p65.

Zusammenfassung

Das angeborene Immunsystem ist die erste Verteidigungslinie gegen eindringende Krankheitserreger. Aufspürung von konservierten „pathogen-associated molecular patterns“ (PAMP) durch „pattern recognition receptors“ (PRR), initiiert die angeborene Immunantwort. Abhängig vom Rezeptor und der Art des PAMP, werden eine Vielzahl von Signalkaskaden aktiviert, was zu einer transkriptionellen Aktivierung von verschiedenen Genen führt. Diese Gene regulieren die Entzündungsreaktion und die angeborenen Wirtsabwehr. *Listeria monocytogenes* ist ein fakultativ intrazelluläres Bakterium, welches in der Lage ist, dem Phagosom ins Cytoplasma zu entweichen, wo es replizieren kann. *L. monocytogenes* wird zuerst durch PRR an der Zelloberfläche erkannt, was den „nuclear factor κB“ (NFκB) Signalweg und die Expression von NFκB-abhängigen Genen aktiviert. Nachdem der Erreger dem Phagosom entkommen ist, wird er durch cytoplasmatische Sensoren erkannt, welche die „interferon response factor 3“ (IRF3) -abhängige Expression und Sekretion von Typ-I-Interferone (IFN) induziert. Typ I Interferone binden wiederrum IFN-α Rezeptorkomplexe (IFNAR), die den „Janus kinase/signal transducers and activators of transcription“ (JAK/STAT) Signalweg aktivieren. Dies führt zur Bildung des „interferon-stimulated gene factor 3“ (ISGF3) komplex und zur Expression von Interferon-abhängigen Genen (ISG). Hier erzeugen und charakterisieren wir einen monoklonalen Antikörper gegen eine der Untereinheiten von ISGF3, nämlich IRF9. Wir zeigen, dass dieser Antikörper ein wertvolles Werkzeug ist um ISGF3 Interaktion mit Chromatin zu studieren.

Im Gegensatz zu klassischen NFκB- oder IFN-abhängigen Genen, brauchen koregulierte Gene, einschließlich jenes Gen das für die „Nitric oxide synthase 2“ (*Nos2),* eine koordinierte Zusammenführung der Transkriptionsmaschinerie die sowohl von NFκB als auch von ISGF3 abhängig ist. Die Behandlung von Knochenmark Makrophagen (BMDMs) mit Hitze-inaktivierten Listerien (hkL) und IFN-β, aktiviert den NFκB und IFN-Signalweg. Diese Kostimulierung ähnelt einer Infektion mit lebenden Listerien.

In dieser Studie wurde die Ausführbarkeit dieser Herangehensweise für das Studieren transkriptioneller Aktivierung von koregulierten Genen gezeigt. Sowohl hkL als auch der klassische NFκB Aktivator „tumor necrosis factor α“ (TNF-α), synergieren mit Typ I IFN bei der Expression von koregulierten Genen, obwohl hkL

höhere Induktionsraten im Vergleich zu TNF-α hervorrief.

Die Rekrutierung des allgemeinen Transkriptionsfaktors TFIIH, inklusive seiner CDK7 („cyclin-dependant kinase 7) Kinase Untereinheit, an den *Nos2* Promotor ist abhängig von NFκB. Im Zuge dieser Arbeit wurden CDK7 und p65 ko-immunpräzipitiert. Dies ist ein Hinweis darauf, dass die Rekrutierung von TFIIH/CDK7 zum *Nos2* Promotor das Ergebnis einer direkten Interaktion zwischen der NFκB Untereinheit p65 und CDK7 ist. Weitere Experimente werden benötigt um dies zu bestätigen. Unerwarteter Weise konnte eine Interaktion zwischen IRF9 und p65 gezeigt werden. Die Funktion dieser Wechselwirkung ist jedoch unklar.